E614 Alignment Monitoring System
(Preliminary design)

George Price, University of Alberta

Contents

1 PREFACE

The following report summarizes my work undertaken during the summer of 1999 at the University of Alberta. This work should be viewed, however, as a work in progress, since I expect to persue aspects of the alignment system over the 1999-2000 academic year and beyond.

I would like to express my appreciation to the Research Corporation for funding which enabled me to undertake this project.

2 BACKGROUND

A system consisting of a laser, pinhole, and CCD-camera was proposed for monitoring the position of the E614-detector. The diffraction pattern produced by light passing through the pinhole is captured by the CCD-camera. The center of the diffraction pattern is calculated and used as an estimate for the position of the pinhole. The pinhole could be mounted in the ends of the four protruding arms shown in the figure-1. A possible layout for the laser, pinhole, and CCD-camera is viewed in figure-2. In figure-2, the laser is mounted on one end of the iron housing surrounding the detector, and the CCD-camera is mounted on the other end. It was suggested

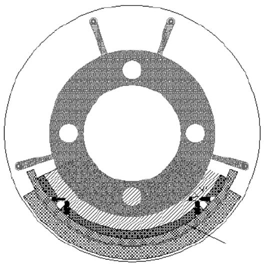

Figure 1: G10 End-plate

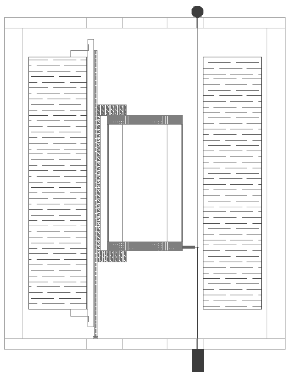

Figure 2: Layout of detector with single laser alignment set

that four such laser-pinhole-CCD camera systems be installed on the detector. With two pinholes mounted on the upstream end of the detector stack and two on the downstream end. Such a system would over-determine the orientation of the detector in the X-Y plane.

This report takes the first step towards a final design. Over the summer a prototype laser, pinhole, and CCD-camera were tested in the lab. Methods to estimate the center of the pinhole based on the diffraction pattern detected were developed. The accuracy of the system with various sizes of pinholes and CCD-camera settings were investigated. Recommendations are made for camera and laser settings as well as pinhole size.

This report does not represent a "finished-product". It summarizes the work performed and additional work yet to be done. The methods developed will need further refinement depending on the final orientation of the system. With this in mind, I've proposed additional tests and changes to the methods developed. I've tried to include sufficient detail so if testing were halted for some time than the report would allow one to get up to speed quickly and continue with testing. Eventually, I imagine this report becoming a manual with detailed description on: software, hardware, installation procedures, Calibration, and operation.

EXPERIMENT E614 AT TRIUMF:
MONITORING DETECTOR ALIGNMENT

The following report examines an alignment monitoring system for the E614-detector. Essentially, a semiconductor laser is passed through a beam-expander to produce a larger cylindrical beam. The laser beam illuminates a circular aperture or (pinhole) mounted within the detector. Light leaving the pinhole falls on a CCD-camera with lens removed. The position of the pinhole is estimated by calculating the center of the intensity distribution captured by the camera. A laser, pinhole, and CCD-camera system are tested in the lab for overall sensitivity to pinhole movement. Recommendations are made for camera settings, methods for finding the pinhole-center, and pinhole radius. Finally, techniques for estimating the center of the pinhole will be integrated into the camera's source code and eventually interfaced with Tool-Command-Language or "TCL".

3 APPARATUS

Its planned, that pinholes will be mounted in the upstream and downstream ends of the detector stack. While testing, the camera was fixed in one position and the pinhole placed in either the upstream or downstream positions (see figure-3).

LAB SETUP

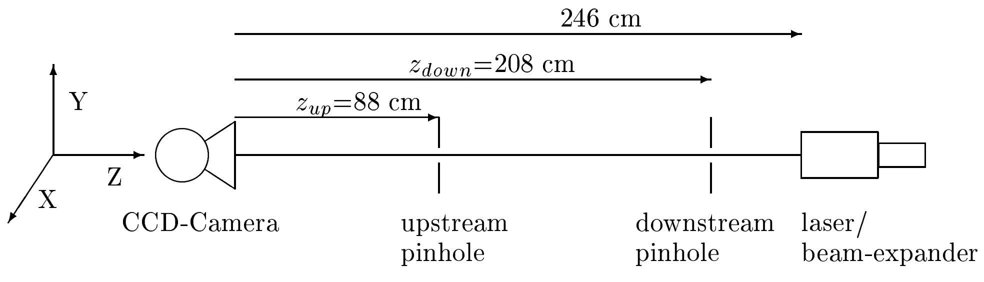

Figure 3: Camera, Pinhole and Laser configuration

Models of equipment used are listed below:

CCD-Camera Make-CONNECTIX QCAM, 320x240 pixel capture, 6-bit gray scale, powered by keyboard port of computer.

Pinhole (3.5 cm x 1.5 cm x 0.18 mm-thick) pieces of aluminum with holes drilled in the middle.

Laser Make-COHERENT, Type-Class (3 a), slot-laser, 5 mW, 670 nm.

Beam-expander Make-Unknown, Diameter-3 cm

Polarizing Filters Make-,Diameter-

When testing, the pinhole was mounted on a sliding platform and camera fixed in one position. The platform was moved parallel to the test bench with accuracy of $\pm 1\mu$m. Most testing consisted of taking pictures of the pinhole in various locations. A change in position of the pinhole was estimated from pictures taken and compared with the actual change in position of the sliding platform.

4 THEORY

While testing, the laser wavelength was 670 nm and the distance from the camera to the upstream and downstream pinholes were 88 cm and 208 cm respectively. Pinhole radii varied from 0.28 mm to 1.18 mm. With the above dimensions the light passing through the pinhole experiences Fraunhofer diffraction (as described in equations 2 and 3). Equation-1 determines the diffraction pattern intensity as a function of radial distance from the Z-axis (see figure-3). Equation-2 is used to find the peak intensity of the diffraction pattern along the Z-axis.

$$I(x) = \left(\frac{J_1(x)}{x}\right)^2 where\, x(r) = \frac{2\pi ar}{\lambda} \tag{1}$$

$$I(z) = \frac{1}{2}\left(\frac{1-\cos(\frac{\pi a^2}{\lambda z})}{\lambda^2}\right) \tag{2}$$

Where:

I = Intensity of light.

J_1 = 1^{st} order Bessel function.

a = Radius of pinhole.

r = Radial distance from center of pinhole.

z = Distance from pinhole to camera along Z-axis.

λ = Wavelength of laser.

Equation-3, the basic "centroid" formula, is used to find the X-coordinate of the Intensity-distribution-center. The error in the X-coordinate of the centroid, equation-4, is found by applying standard error analysis (e.g. taking the partial derivative of equation-3 with respect to "n_2" and "$I(n_1, n_2)$" , multiplying by respective errors in n_2 and I, adding all terms in quadrature, and taking the square-root. The Y-position and error is found by replacing all "n_2" with "n_1".

- Note, from now on, I refer to this method for estimating the center of the pinhole as the "centroid" method.

$$X_{cen} = \frac{\sum_{n_1=1}^{N_1} \sum_{n_2=1}^{N_2} n_2 I(n_1, n_2)}{\sum_{n_1=1}^{N_1} \sum_{n_2=1}^{N_2} I(n_1, n_2)} \tag{3}$$

Letting:

$s_I = \sum_{n_1=1}^{N_1} \sum_{n_2=1}^{N_2} I(n_1, n_2)$

$s_I^2 = \sum_{n_1=1}^{N_1} \sum_{n_2=1}^{N_2} (I(n_1, n_2))^2$

$s_X = N_1 \sum_{n_2=1}^{N_2} n_2$

$s_X^2 = N_1 \sum_{n_2=1}^{N_2} (n_2{}^2)$

$s_{XI} = \sum_{n_1=1}^{N_1} \sum_{n_2=1}^{N_2} n_2 I(n_1, n_2)$

$$\delta X_{cen} = \sqrt{\frac{\delta n_2{}^2 s_I^2}{(s_I)^2} + \frac{\delta I^2}{(s_I)^4}\left[(s_I)^2 s_X^2 - 2 s_{XI} s_I s_X + N (s_{XI})^2\right]} \tag{4}$$

Where:

X_{cen} = X-coordinate of centroid in pixels.

δX_{cen} = Error in X-coordinate of centroid in pixels.

N_1 = Total height of picture in pixels.

N_2 = Total width of picture in pixels.

n_1 = Y-coordinate of each pixel in units of pixels.

n_2 = X-coordinate of each pixel in units of pixels.

$I(n_1, n_2)$ = Intensity of each pixel with units of 0-63 gray-scales.

δn_2 = Error in X-coordinate for each pixel.

δI = Error in Intensity for each pixel.

To remove noise, such as dust on the CCD-array or beam expander, all pictures were filtered. Filtering is accomplished by taking the two dimensional Discrete Fourier Transform or DFT (see equation-5). Low-pass filtering was performed by setting all frequency components greater than some minimum[1] frequency to zero.

$$F(k_1, k_2) = \sum_{n_1=0}^{N_1-1} \sum_{n_2=0}^{N_2-1} I(n_1, n_2) exp\left[-j\frac{2\pi}{N_1}n_1k_1 - j\frac{2\pi}{N_2}n_2k_2\right] \tag{5}$$

Where:

$F(k_1, k_2)$ = DFT at frequencies "k_1" and "k_2".

$I(n_1, n_2)$ = Intensity of each pixel.

N_1 = Height of image in units of pixels.

N_2 = Width of image in units of pixels.

k_1 = Y-coordinate in frequency domain.

[1] The magnitude of the DFT spectrum is highly localized. High frequency components soon approach zero and contribute little to rebuilding the image. For an ideal spherical Bessel function, which is close in shape to the actual image detected with the camera, the high frequency components are zero. Thus, high frequency components close to zero in magnitude were likely caused by dust on the CCD-array or digitization noise and were set to zero (see figures 19, 25, 31 and 37) in appendix-B.

k_2 = X-coordinate in frequency domain.

n_1 = Y-coordinate in spatial domain.

n_2 = X-coordinate in spatial domain.

Another way to monitor the position of the pinhole is by tracking the phase-shift of "$F(k_1, k_2)$" corresponding to a shift in position of the pinhole. For a one-dimensional signal of length "N", shifting it by "m" results in a phase-shift of the DFT by $\left(\frac{2\pi km}{N}\right)$.[2] As a result, there is a linear relation between the change in pinhole-position and change in phase. For the experiment in question the phase of $F(1,0)$ and $F(0,1)$ were tracked to estimate the change in position of the pinhole center in the "X" and "Y" directions (see equation-6) . The phase-error in the X-direction is found by applying standard error analysis (e.g. setting k_1 to zero, taking the partial derivative of equation-6 with respect to "$I(n_1, n_2)$", "n_2", multiplying by "δI", " δn_2" respectively, adding all terms in quadrature, and taking the square root) see equation-7. The Y-phase error was found by setting "k_2" to zero and replacing "k_1" and "δn_2" with "k_1" and "δn_2" in equation-7.

- Note, from now on, I refer to this method for estimating the center of the pinhole as the "phase-shift" method.

Letting:

$s_X = \sum_{n_1=0}^{N_1-1} \sum_{n_2=0}^{N_2-1} I(n_1, n_2) \cos\left(\frac{2\pi k_1 n_1}{N_1} + \frac{2\pi k_2 n_2}{N_2}\right)$

$s_Y = \sum_{n_1=0}^{N_1-1} \sum_{n_2=0}^{N_2-1} I(n_1, n_2) \sin\left(\frac{2\pi k_1 n_1}{N_1} + \frac{2\pi k_2 n_2}{N_2}\right)$

$$\theta = \arctan\left(\frac{-s_Y}{s_X}\right) \tag{6}$$

$$\delta\theta = \sqrt{\frac{N_1 N_2 \delta I^2}{(s_X)^2 + (s_Y)^2} + \delta n_2{}^2 \left(\frac{2\pi k_2}{N}\right)^2} \tag{7}$$

[2]Phase and error-in-phase in equations 6 and 7 are converted to units of pixels by multiplying by $\left(\frac{N}{2\pi k}\right)$ where "N" can equal N_1 or N_2 depending on whether the "X" or "Y" positions of the pinhole-center are tracked.

Where:

θ = Phase of Discrete Fourier Transform.

$\delta\theta$ = Error in X-phase.

N_1 = Height of picture in pixels

N_2 = Width of picture in pixels

n_1 = Y-coordinate of pixel in spatial domain.

n_2 = X-coordinate of pixel in spatial domain.

$I(n_1, n_2)$ = Intensity of pixel.

k_1 = Y-coordinate in frequency domain.

k_2 = X-coordinate in frequency domain.

δn_2 = Error in X-direction.

δI = Error in Intensity.

5 DESIGN CONSIDERATIONS

Choosing a reasonable pinhole radius, CCD-camera settings, and method for estimating the center of the pinhole requires consideration of several factors. A list of factors which will effect final choices are summarized bellow:

1. **Distance of Pinhole from camera**
   - For a given laser-wavelength and distance from CCD-camera to pinhole, the pinhole radius which gives peak intensity at the camera is found with equation-2 by letting $\left(\frac{a^2}{\lambda z} = 1\right)$.
   - Any radii different from those calculated with equation-2, by letting $\left(\frac{a^2}{\lambda z} = 1\right)$, will reduce the peak intensity of the diffraction pattern detected.
2. **Error in Pinhole-position**

- To minimize error in pinhole-position the pixel intensities should be increased as large as possible without exceeding the maximum allowable gray-scale level of the camera. In addition, making error-in intensity, δI, and error-in X-position of each pixel, δn_2, as small as possible will reduce overall error.
- Factors effecting pixel-intensity-error are:

  Digitization error: Pixels are assigned gray-scale levels, depending on intensity, from 0 to 63. All pixel intensities are rounded up or down to the nearest neighboring level. This action introduces an error of ± 0.5 gray-scale-levels.

  Random Pixel Intensity Variation: Tests were performed where light was blocked from the camera and the standard deviation of the pixel intensities calculated. I found the standard deviation was dependent on the brightness-level of the CCD-camera[3]. For brightness-levels used in the lab this random error was approximated at ± 1 gray-scale-levels.
- To estimate the pixel-position-error the following logic was used.

  Error in Pixel Position: For calculations of the pixel location its assumed that the center of each pixel corresponds to its geometric center. In reality, the intensity varies over each pixel, shifting the centroid of the pixel away from its geometric center. I show later that pixels with intensities equal to or greater than five gray-scale levels will have an error in pixel position estimated at ± 0.02 pixels.

3. **Effects of changing pinhole radius**[4]

   - Increasing pinhole radius has the following effects:
     - The central peak of diffraction pattern will narrow.
     - The shape of the diffraction pattern starts to diverge from what is predicted by Fraunhofer diffraction in equation-1.

[3] Brightness-level is similar to shutter speed for a conventional camera.

[4] In both cases the pinhole radius is changed from the one which gives the greatest peak intensity (as calculated from equation-2 by setting $\frac{a^2}{\lambda z}=1$).

  - The shape of the new diffraction pattern is composed of more high frequency components. Making removal of high frequency noise more difficult. Since good-signal is thrown out with the bad-signal.
- Decreasing pinhole radius has the following effects:
  - The central peak of the diffraction pattern widens.
  - The shape of the diffraction pattern more closely approximates Fraunhofer diffraction predicted by equation-1.
  - DFT is more localized making low-pass filtering more effective.

4. **Image collection speed**

- The following camera settings influence the speed with which the pinhole center may be tracked:
  (a) Transfer-scale (picture resolution)
    - There are three choices of transfer-scale:

      transfer-scale=1 Every pixel is used.

      transfer-scale=2 Every other pixel is used. Reducing total pixels by four.

      transfer-scale=4 Every fourth pixel is used. Reducing total pixels by sixteen.

  (b) Picture size
    - There are three choices of picture-size:

      window 1 = 240x320 pixels.

      window 2 = 120x160 pixels.

      window 3 = 60x80 pixels.
- Choosing a larger transfer-scale or smaller window will decrease the time between successive pictures. But, will increase error in estimating the center of the pinhole.
- Increasing brightness-level is similar to increasing exposure time for a regular camera. It was found that brightness levels less "120" should be used to make the "exposure" time insignificant.

Next I consider the above points in more detail.

5.1 Distance of Pinhole from Camera

While testing the distance from the camera to the pinhole, in either the upstream or downstream positions, matches what they actually will be for the E614 detector (see figure-3). As viewed in figure-3 the distances from the pinhole to the camera, in the upstream and downstream positions, are listed below:

upstream distance $= z_{up} = 88$ cm

downstream distance $= z_{down} = 208$ cm

laser-wavelength $= \lambda = 670$ nm

Substituting $\left(\frac{a^2}{\lambda z} = 1\right)$ into equation-2 will find the peak intensity of the diffraction pattern. Inserting "z_{up}" or "z_{down}" and "λ" into $\left(\frac{a^2}{\lambda z} = 1\right)$ determines the radii "a_{up}" and "a_{down}" required to produce peak intensity[5] of the diffraction pattern. The corresponding radii are summarized below:

$a_{up} = 0.768$ mm

$a_{down} = 1.18$ mm

Any shift in radius from "a_{up}" and "a_{down}" will reduce peak intensity.

5.2 Error in Pinhole Position

Minimizing error in pinhole position is of highest priority. Closer inspection of equations 4 and 7 provide clues on what shape of diffraction pattern produces minimum error. Conditions for minimum and maximum error in equations 4 and 7 are listed below.

- **For minimum error**
  1. In equation-4
     (a) $I(n_1, n_2) = I$
     (b) $n_1 = n_2 = n$
     (c) $N_1 \to \infty$
     (d) $N_2 \to \infty$
     (e) $I(n_1, n_2) \to \infty$

[5] The expression $\left(\frac{a^2}{\lambda z} = 1\right)$ assumes zero divergence of the laser

(f) $\delta I \to 0$

(g) $\delta n_2 \to 0$

2. In equation-7

(a) $I(n_1, n_2) \propto \cos\left(\frac{2\pi k_1 n_1}{N_1} + \frac{2\pi k_2 n_2}{N_2}\right)$ or $\sin\left(\frac{2\pi k_1 n_1}{N_1} + \frac{2\pi k_2 n_2}{N_2}\right)$

(b) $I(n_1, n_2) \to \infty$

(c) $N_1 \to \infty$

(d) $N_2 \to \infty$

(e) Choose k_2 such that ($F(0, k_2)$ is maximum) to minimize error in X-direction.

(f) Choose k_1 such that ($F(k_1, 0)$ is maximum) to minimize error in Y-direction.

(g) $\delta I \to 0$

(h) $\delta n_2 \to 0$

- **For maximum error**

1. In equation-4

(a) $I(n_1, n_2) \neq I$

(b) $n_1 \neq n_2 \neq n$

(c) $N_1 \to 0$

(d) $N_2 \to 0$

(e) $I(n_1, n_2) \to 0$

(f) $\delta I \to \infty$

(g) $\delta n_2 \to \infty$

2. In equation-7

(a) $I(n_1, n_2) = I$

(b) $I(n_1, n_2) \to 0$

(c) $N_1 \to 0$

(d) $N_2 \to 0$

(e) $\delta I \to \infty$

(f) $\delta n_2 \to \infty$

We see increasing "$I(n_1, n_2)$", "N_1" and "N_2" while decreasing "δI" and "δn_2" will reduce error in both equations 4 and 7.

In equation-4 the constraint $n_1 = n_2 = n$ is another way of saying that infinite pixel density minimizes error. For example, as

$n_1 \to \infty$ then n_1 will equal $(n_1 + 1)$ matching are constraint. Thus, the condition that $n_1 = n_2 = n$ implies a localized intensity-distribution while the additional condition $n \to \infty$ requires the intensity distribution has a large number of pixels. This can be visualized by considering an Intensity distribution confined between minimum and maximum pixel locations; N_{min} and N_{max}. To minimize error we require $\frac{N_{max}-N_{min}}{N_{min}}$ and $\frac{N_{max}-N_{min}}{N_{max}} \ll 1$ and $N_{max} - N_{min} \to \infty$. The ideal compromise would be a highly localized intensity distribution confined within a very high pixel density window.

In equation-6 "k_1" and "k_2" are chosen to give maximum $F(0, k_1)$ and $F(k_2, 0)$ to minimize error[6]. For tests performed the dominant spatial frequencies were (k_1=0,k_2=1) for the X-direction and (k_1=1,k_2=0) for the Y-direction. When considering "maximum-error"; a major difference between equations 4 and 6 is noticed. The condition $I(n_1, n_2) = I$ helps to minimizes error in equation-4 but maximizes error in equation-6. However, this condition is true, only if all pixels are of the same intensity "I". In this case equation-6 more accurately describes the physical situation. If all pixels within the camera window are of equal intensity than there's no way to predict the outer boundaries of the intensity distribution and no way to find its center. As a result error should go to infinity as predicted by equation-6. Conversely, equation-4 estimates the center of the intensity distribution at the center of the picture window with some finite error. But, this is meaningless since the boundaries of the intensity distribution are undefined.

5.2.1 Estimating Error in Pixel Intensity

There are two major effects which cause error in pixel intensity:

1. **Digitization Error**

[6]Note, for "k_1" and "k_2" the phase shift may exceed (2π-radians) if the image is shifted by more then ($\frac{N}{2}$). As a result the diffraction pattern would start to repeat. To avoid this I've chosen harmonics (k_1=0,k_2=1) and (k_1=1,k_2=0) which will not suffer this problem. These harmonics are largest next to, (k_1=0,k_2=0), the"DC" component. However, the "DC" component cannot relate any information on phase because its phase is zero. Therefore, the harmonics chosen are the largest ones possessing phase information. As a result they are the best choice for minimizing error (see conditions "for minimizing error") and won't suffer from the phase repeating itself

Brightness Level	I_{avg}	σ_I	Percentage of pixels within one of I_{avg}
0	4.24	0.70	97.7
20	4.27	0.64	98.1
40	4.23	0.60	98.9
60	4.23	0.56	99.0
80	4.30	0.58	98.6
100	4.48	0.67	96.9
120	4.62	0.67	97.7
140	4.87	0.69	98.0
160	5.35	0.72	96.8
180	6.26	0.72	97.2
200	8.51	0.87	92.4
220	13.37	1.15	89.0
240	24.68	1.81	73.4

Table 1: Where, "I_{avg}" equals the average pixel intensity and "σ_I" is the corresponding standard-deviation. Both "I_{avg}" and "σ_I" are in units of gray-scale level . Percentage-of-pixels-within-one-of-I_{avg} were found by rounding "I_{avg}" to the nearest gray scale level and counting the number of pixels within one gray scale level of the rounded-I_{avg}. Note each pixel is assigned a gray scale level from 0 to 63.

- For the camera used all intensity levels were assigned numbers between 0-63. Pixels with intensities in between levels will be rounded to the nearest neighboring level. Thus, an intensity error of "0.5" is introduced by the act of digitization.

2. **Random fluctuations of pixel intensities**

   - If the CCD-camera were perfect; blocking light to it would result in all pixels having the same intensity. In reality, some pixels deviate from the average. Pictures were taken, with light blocked from the camera, for various brightness levels. Table-1 summarizes these results.
   - Note brightness level is like shutter speed for a conventional camera. A slow shutter speed corresponds to a large brightness level.

Notice from table-1 that the vast majority of pixels have intensities within one gray-scale level of the average. Only for brightness levels greater than "200" is this not true. As long as the brightness levels are less than "200"; a conservative estimate for random fluctuations of intensity is ± 1 gray-scale levels. Assuming both sources of error are random in nature than the combined error can be found by adding the two in quadrature. Leading to a combined error of "1.1" or approximately "1" gray-scale level.

5.2.2 Error in Pixel position

Error in pixel position is caused by two factors:

1. **Variation of actual diffraction pattern over a pixel.**
2. **Variation in size of pixels.**

To investigate the first factor I consider figure-4 ; which shows the theoretical diffraction patterns for the upstream and downstream pinholes. The variation of the diffraction pattern over one pixel may be estimated by the slope of the two patterns. For both patterns in figure-4 the greatest variation of the diffraction pattern is along either side of the central maximum. For the narrow pattern the slope equals approximately the height of diffraction pattern in gray-scale levels divided by half the width of the central peak. I assume the height of the diffraction pattern equals the maximum gray-scale level of 63. By this assumption I maximize the slope and hence the variation of intensity over one pixel. Making my estimate as conservative as possible. The width of the narrow diffraction pattern is approximately "146" pixels, thus its slope equals $\frac{(2)63}{146}$=0.863 gray-scale levels per pixel. The centroid of a pixel can be calculated using the intensity variation found from the slope calculated earlier. If this calculation is performed for pixels with intensities greater than five gray scale levels the actual pixel center is less than 0.02 pixels from its geometrical center. The vast majority of pixels within the central peak of the diffraction pattern have intensity greater the five gray-scale level. For these pixels the deviation of the centroid is less than 0.02 since more gray-scale levels "weight" the centroid of the pixel towords its geometric center. While the intensiy variation outside the central maximum is almost minimal and shouldent contribute significantly.

The second factor, variation in size of pixels, depends on the quality of fabrication of the CCD array. For this case error is added to the absolute position of the diffraction pattern. To simplify things I assume this effect contributes negligibly to random-error in the position of the diffraction pattern.

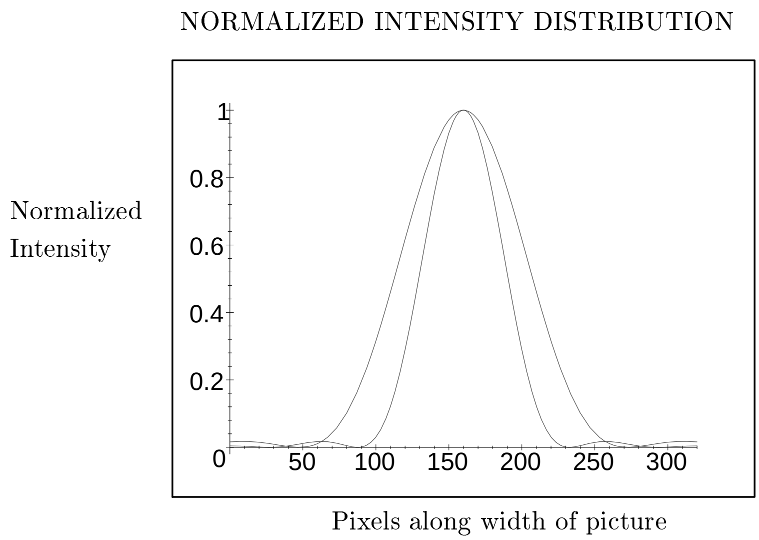

Figure 4: The above curves are the theoretical diffraction patterns for the upstream and downstream diffraction patterns. The "narrow" curve corresponds to the upstream pinhole a_{up}=0.495 mm and z_{up}=88 cm. While the "wider" curve corresponds to the downstream pinhole at a_{down}=0.755 mm and z_{down}=208 cm (see figure-3). For both cases the wavelength, λ=670 nm.

5.3 Effects on changing Pinhole radius

The effects of changing pinhole radius on the diffraction patterns detected are seen in figures 5, 6, 7, and 8. The solid line corresponds to the theoretical-diffraction-pattern, found by equation-1, and the "cross" pattern corresponds to the measured-diffraction-pattern. All measurements were taken at z_{up}=88 cm (see figure-3). In this position the pinhole radius which gives peak intensity is found in section-3.1 and equals 0.768 mm. As expected, reducing the pinhole diameter widens the measured diffraction pattern. However, for the larger pinholes shown in figures 5 and 6 we see the measured and ideal diffraction patterns diverge. I suspect the added "shoulders" on the measured diffraction patterns are caused by divergence of the laser. A 6.5 mrad divergence was measured for the laser and beam expander combination. For larger pinholes there will be as significant difference in phase between light passing through the pinhole-center compared with light passing near the pinhole-edge. A quick calculation of the phase difference for various pinholes is summarized below.

Pinhole Radius in mm	Phase Difference in degrees
1.185	18.4
0.755	7.4
0.498	3.2
0.286	1.1

Table 2: Using geometry, the phase difference of light passing through the center and outer edge of pinholes is calculated. All pinholes were located in the upstream position corresponding to z_{up} equaling 208 cm (see figure-3. X-sections of the diffraction patterns produced by the above pinholes are seen in figures 5, 6, 7, and 8

Ultimately, if tests were performed with a non-diverging laser and the "shoulders" on the diffraction patterns disappear; than we would be confident that the distorted diffraction patterns were caused by divergence of the laser.

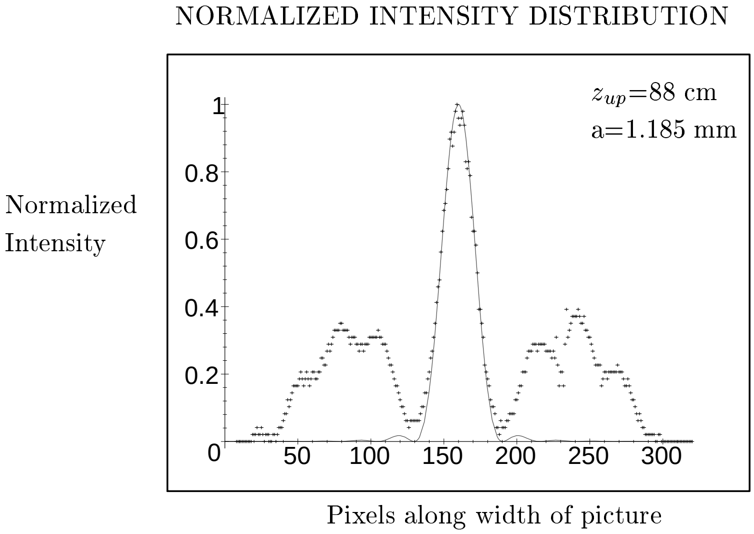

Figure 5: The solid line is the theoretical diffraction pattern and the "cross" symbol is the measured diffraction-pattern-X-section for z_{up}=88 cm (see figure-3). The wavelength of light, λ, equals 670 nm. Both curves were normalized to Intensity level=1. Each curve corresponds to a pinhole radius of a=1.185 mm

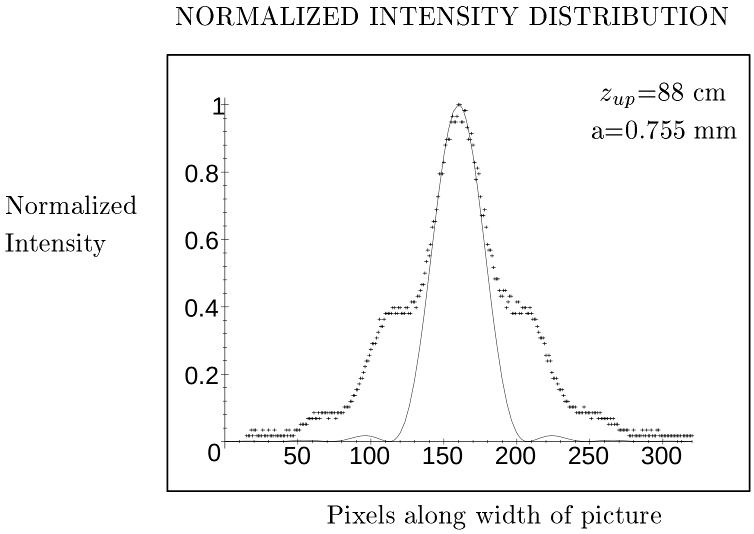

Figure 6: The solid line is the theoretical diffraction pattern and the "cross" symbol is the measured diffraction-pattern-X-section for z_{up}=88 cm (see figure-3). The wavelength of light, λ, equals 670 nm. Both curves were normalized to Intensity level=1. Each curve corresponds to a pinhole radius of a=0.755 mm

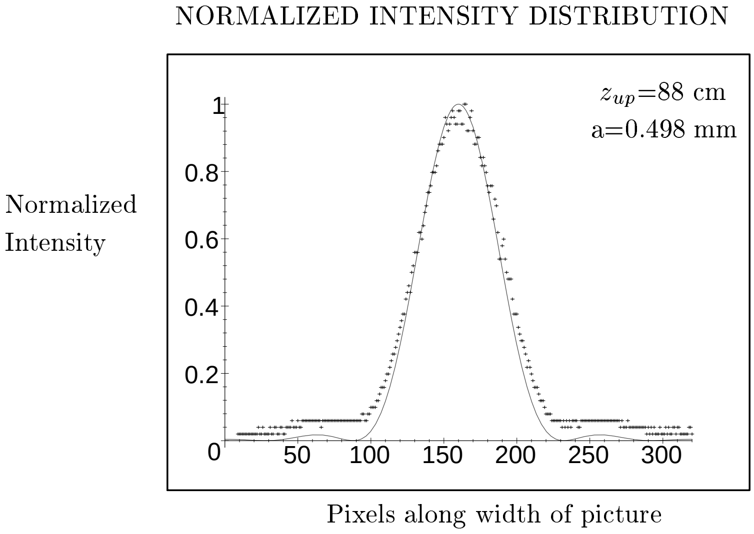

Figure 7: The solid line is the theoretical diffraction pattern and the "cross" symbol is the measured diffraction-pattern-X-section for z_{up}=88 cm (see figure-3). The wavelength of light, λ, equals 670 nm. Both curves were normalized to Intensity level=1. Each curve corresponds to a pinhole radius of a=0.498 mm

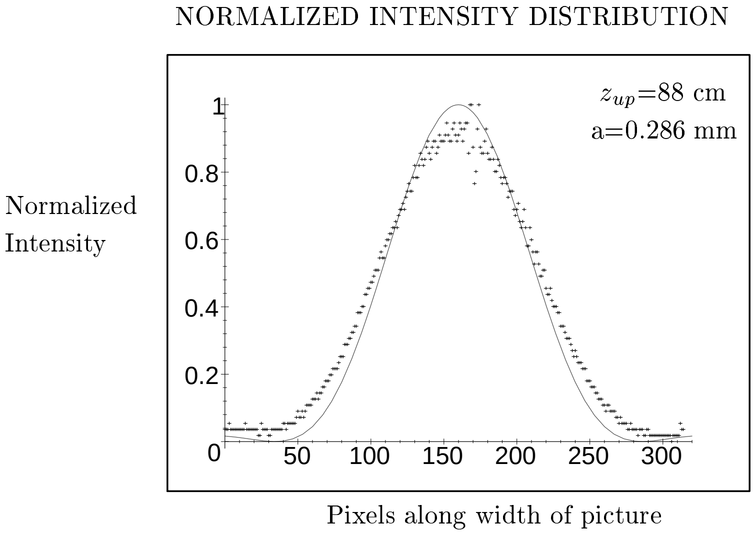

Figure 8: The solid line is the theoretical diffraction pattern and the "cross" symbol is the measured diffraction-pattern-X-section for z_{up}=88 cm (see figure-3). The wavelength of light, λ, equals 670 nm. Both curves were normalized to Intensity level=1. Each curve corresponds to a pinhole radius of a=0.286 mm

Effects on changing the pinhole radius are summarized below.

1. **Larger Pinholes**
   - For the upstream case pinholes larger than a=0.768 mm will have a reduced peak intensity given by equation-2.
   - The central peak is narrowed.
   - With larger pinholes the diffraction pattern is distorted from what theory predicts. This might be caused by divergence of the laser.
   - The new shape of the diffraction pattern requires more high frequency components to reconstruct. Making it more difficult to separate unwanted high frequency noise from the desired signal.
2. **Smaller Pinholes**
   - For the upstream case pinholes smaller than a=0.768 will have reduced peak intensity as given by equation-2.
   - The central peak is widened.
   - Smaller pinholes diffract light similar to what Fraunhofer-diffraction predicts. As a result the intensity distribution is similar to an ideal Bessel function and is highly localized in the frequency domain. In this way the high-frequency noise can be removed without effecting the original signal.

5.4 Image Collection Speed

The CCD-camera used has great flexibility on image size (e.g. height and width of picture) as well as pixel resolution (e.g. use every pixel, every other pixel or every fourth pixel). Image size and resolution directly effect the amount of data the camera transfers for each picture. As a result the speed with which the center of the diffraction pattern can be found is faster for smaller pictures of low pixel resolution. As a consequence, estimating the center of the diffraction pattern quickly might allow detection of vibrations. However, accuracy is lost when using lower pixel resolution since the effective pixel size is double if every other pixel is used four times as large if every fourth pixel is used.

- **Note:** When I say every second pixel is used, I mean pixels are used from every other column and every other row. This means the total number of pixels used to make the image is reduced by four. Similarly, if pixels are used from every fourth column and fourth row the total number of pixel used to make the image is reduced by sixteen.

One implication of smaller window sizes is part of the diffraction pattern may be off the picture window. [7].

Image collection speed is also effected by the brightness-level used. Brightness-level effects the exposure time of the picture (e.g. long exposure time corresponds to large brightness-level). To test this a thousand pictures were taken in succession and the total time recorded (see table-3). As viewed in table-3 the effect of brightens-level on picture time becomes significant for levels greater than "100". Therefore, to minimize the time needed to take a picture brightness levels less than 120 should be used.

Transfer Scale	Brightness level	Time of Run (s)
4	0	52
4	20	53
4	40	54
4	60	53
4	80	53
4	100	54
4	120	55
4	140	57
4	160	64
4	180	81

Table 3: One thousand pictures were taken is succession for various brightness levels. The time for each run was recorded in units of seconds with accuracy of ± 0.5 seconds.

[7]If a large part of the diffraction pattern is off the picture then accuracy is drastically reduced. Since much of the data used to calculate the center of the diffraction patterns is no longer present.

6 PROPOSED DESIGN 1^{st} DRAFT

. In this section the position monitoring system developed for testing[8]in the lab is examined. The following subjects are covered:

1. **Design Description**
2. **Choice of Pinhole Radii**
3. **Software**
4. **System Setup and Operation**

6.1 Design Description

I envision the final system design to work as follows:

- The laser and beam expander are mounted on one end of the detector and the CCD-camera at the other end. A pinhole is mounted somewhere along the detector stack[9]. Once the system is mounted on the detector appropriate camera settings are found to produce maximum intensity at the camera so as to minimize error.
- Tool-Command-Language or "TCL" will instruct the CCD-camera to take a picture. At the same time the software added to the source code of the CCD-camera will estimate the center of the pinhole, its error, and total sum of all pixel intensities. Initially "TCL" will specify that both centroid and phase-shift methods be used to estimate the absolute position, phase, and errors of the pinhole.
- Once the initial position of the pinhole is found and recorded; "TCL" will specify that future pictures be found using only the phase-shift method.
- "TCL" will than record the position of the pinhole at regular intervals and time stamp the data. In this way, the position of the detector is tracked with respect to time.

[8]For testing the system described in this section was used. Its expected that the final system will be different. But, the methods for estimating the center of the pinhole, pinhole-radius, and camera settings should be similar no matter what the final design.

[9]For testing, distances corresponding to upstream and downstream ends of the detector stack were used (see figure-3)

- Finally, drastic variations in pinhole position could be flagged to alert people of possible alignment changes.

6.2 Choice of Pinhole Radii

Choices for pinhole radii were:

1. **Upstream Pinhole** a_{up}=0.495 mm
2. **Downstream Pinhole** a_{down}=0.755 mm

Figure-9 shows X-sections of the diffraction patterns measured for the two choices of pinholes in their appropriate upstream and downstream locations. To accept the above pinhole sizes they had to meet

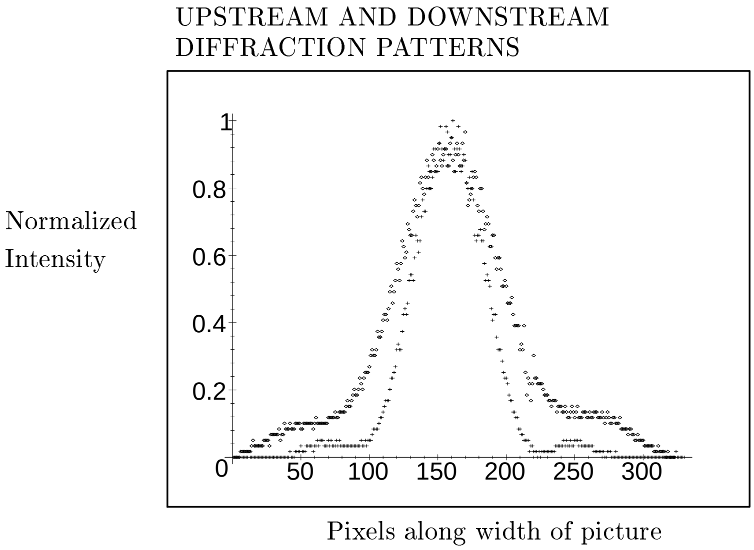

Figure 9: The "cross" pattern is the upstream diffraction pattern with pinhole radius of a_{up}=0.495 mm and z_{up}=88 cm. The "diamond" pattern is the downstream diffraction pattern with pinhole radius a_{down}=0.755 mm and z_{down}=208 cm. For both patterns the laser wavelength is λ=670 nm.

the following criteria:

- Ensure the error in position of the pinhole is small. To make the error in position as small as possible the peak intensity measured by the camera was made as close as possible to the maximum allowable gray scale level (see section-3.2). This was achieved by increasing the brightness-level of the camera. Only pinholes which required brightness-levels less than 180 were considered (see section-3.4).

- Pinholes were chosen small enough so the diffraction patterns detected were similar to what's expected from equation-1 (see section-3.3). As a result the intensity distribution was more localized in the frequency-domain. Making it easier to filter high frequency noise without removing information needed to reconstruct the image.
- Pinholes were sized large enough to ensure the central peak of the diffraction pattern is contained within the camera window. This condition allows using smaller windows to permit taking pictures more quickly.

For the upstream pinhole many different radii will meet the above criteria. I sized this pinhole to keep the central maximum well within the picture window. For the downstream pinhole the distance from the camera to the pinhole was 208 cm. The larger distance allows the diffraction pattern to spread more in the radial direction; making it difficult to confine the central maximum within the picture window. Larger pinholes will narrow the central maximum but distort the pattern detected as seen in figure-5. As a result I chose as large of pinhole as possible to ensure the central maximum of the diffraction pattern was in the picture window but not too large to where the pattern distorts as seen in figure-5.

6.3 Software

The purpose of this section is to introduce software developed to find the center of the diffraction pattern and error in center. The following list shows the software added to the existing source code.

- **qcam.c**
  - filters(scan,q,centroid,fcent) $\longrightarrow$ filters.c
    - f3tensor(1,1,1,h,1,w) $\longrightarrow$ Filter-lib.c
    - rlft3(array2,spec,1,h,w,1) $\longrightarrow$ rlft3.c
    - lowpass(array2,spec,fltr,w,h) $\longrightarrow$ Filter-lib.c
    - fcentroid(array2,q,w,h,cent) $\longrightarrow$ fcentroid.c

The above is a software hierarchy list. To the left of arrow is a C-program-function and to the right of the arrow is the file which the function is contained in. The above list can be summarized in words by saying qcam.c-file contains function filters() and Filter.c-file contains functions f3tensor(), rlft3(), lowpass() and fcentroid()[10]. The file "qcam.c" contains the source code needed by the camera to take a picture. The above functions are defined as follows:

filters(scan,q,centroid,fcent): Function added to "qcam.c" to find the center of diffraction pattern, and error in center, for a picture taken by the CCD-camera.

f3tensor(1,1,1,h,1,w): Function loads picture-data into a two-dimensional array.

rlft3(array2,spec,1,h,w,1): Function finds the Discrete-Fourier-Transform or DFT of picture data. The data loaded into f3tensor() is passed to rlft3() where the Fast-Fourier-Transform algorithm is used to find the DFT.

lowpass(array2,spec,fltr,w,h): Function applies a low-pass filter to the data returned from rlft3(). The inverse DFT is found to reconstruct the filtered image.

fcentroid(array2,q,w,h,cent): Function finds the center and error in center of the filtered data using the centroid method.

Now I examine in depth how these functions and associated programs work.

6.3.1 qcam.c

The file "qcam.c" contains the source code for the CCD-camera used (see appendix A.1). This source code has all the instructions needed to take a picture with the QUICKCAM model of CCD-camera. Essentially, the qcam.c program does the following:

1. Settings such as brightness, white-balance, and contrast are entered on the command line when executing the program. These commands, along with defaults, are sent to the CCD-camera instructing it to take a picture.

[10]Note, I commonly write a C-program-function as "function()", without arguments between brackets, to simplify notation.

2. The CCD-camera takes a picture and assigns each pixel a digitized intensity level from 0 to 63. Intensity levels are converted to binary numbers and sent back to qcam.c.

3. Eventually all binary data composing the picture is sent from the camera back to qcam.c. The data is located in the variable "scan", which is a one dimensional pointer-array. "scan" is made from rows of pixel-data placed side by side resulting in a data array of length , in bytes, equaling the total number of pixel in the image.

4. The data in "scan" is used to find the center of the diffraction pattern captured by the camera.

6.3.2 filters(scan,q,centroid,fcent)

The function filters() is located in file filters.c see–appendix A.2). The filters() function finds the center of the diffraction pattern captured by camera. The arguments of this function are defined as follows.

1^{st} **argument scan:** All data from a picture is located in the scan pointer-array.

2^{nd} **argument q:** All camera settings are stored in the qcam-control-structure or "QCS". These settings such as brightness, contrast, picture size and so-on may be specified on the command line when requesting the CCD-camera to take a picture. All settings have defaults stored in qcam-lib.c which are used if the command line is left blank. "q" is a pointer which can access the various settings within "QCS" by using the command (q→setting).

3^{rd} **argument centroid:** An array which stores all data calculated. This includes:

- X-Phase[11]
- Y-phase
- X-phase error
- Y-phase error
- X-coordinate of diffraction pattern center[12]

[11] All terms with word "phase" are found with phase-shift method

[12] All terms with word "coordinate" are found with centroid method.

- Y-coordinate of diffraction pattern center.
- Error in X-coordinate of diffraction pattern center.
- Error in Y-coordinate of diffraction pattern center.
- Sum of all pixel intensities for filtered data.
- Sum of all pixel intensities for non-filtered data.

4^{th} **argument fcent:** A pointer allocated memory for storing all filtered data.

The purpose of the filters() function is documented in its source code, filters.c, found in appendix- A.2. This is the core program used to find all necessary quantities stored in the "centroid" array. How it works is listed below:

1. **Load Data into 2-D array**

   - The data from a picture is stored in the 1-D pointer-array "scan". To find the DFT the data is loaded into a 2-D array. Appropriate memory is allocated to the 2-D array, named "array2", and the data from "scan" is read in. The DFT algorithm requires a 2-D array of both height and width equal to 2^n, where n is and integer. I chose a square window with maximum size of 256 pixels by 256 pixels. For the case of the largest camera window of size 240 x 320 the corresponding DFT window is 256 x 256. All smaller pictures reduce the camera and DFT windows by a factor of 2^n, where "n" is an integer. As a result of the difference in window sizes some data is lost along each row of the camera window. To avoid having one window off-set from the other; the DFT window is centered over the camera window.

2. **Find DFT**

   - The Discrete Fourier Transform or DFT is found with function rlft3(). The data loaded in "array2" is passed to rlft3() where the Fast Fourier Transform algorithm is used to find the DFT.
   - The DFT is stored back in "array2".

3. **Find Phase**

- The phase is found using equation-6[13]. However, the "s_X" and "s_Y" terms correspond to the "real" and "imaginary" components of the DFT for spatial frequencies "k_1" and "k_2". For our case I chose spatial frequencies with largest magnitude (see section-3.2). These frequencies correspond to (k_1=0,k_2=1), for the X-direction, and (k_1=1,k_2=0), for the Y-direction. Thus, "s_X" and "s_Y" are read directly from the (0,1) and (1,0) terms of the DFT. X-phase and Y-phase are stored in variables "phasex" and "phasey" respectively.

4. **Find Error in Phase**

   - Error in phase is found using equation-7[14]. Again the s_X and s_Y terms are found from the DFT. In filters.c source code, the error-in-x and error-in-y are stored to variables "errorx" and "errory" respectively.

5. **Find Center of Diffraction Pattern Using Centroid Method**

   - Once the phase and phase error are found, the remaining code in "filters.c" is used to find the absolute[15] position of the diffraction pattern. To find the center diffraction pattern using this method the following steps are used:
     (a) A lowpass filter is applied to the DFT, stored in "array2", using function lowpass(). The filtering removes high frequency noise, such as dust spots on the camera or beam-expander.
     (b) The inverse DFT is found. Generating a filtered version of the original image.
     (c) The center of the filtered image is found by function fcentroid() which uses equation-3 and equation-4.

6. **Toggling between Phase and Centroid Methods**

   - Two additional terms were added to the qcam control structure or ("QCS" see definition for "q"-argument from before). These terms are defined below:

[13] Phase is converted to pixels by multiplying by $\frac{N}{2\pi}$ (see discussion just before equation-6).
[14] Error in phase is converted to pixels in the same way as phase (see previous footnote).
[15] The phase-method can determine a relative change in position of the diffraction pattern but not absolute position.

q→filter: Allows changing Filter size on command line.

q→cal: Allows toggling between the phase-shift method for tracking the center of the diffraction pattern or using the centroid method supplied by function fcentroid().

The first term "q→filter" was added to make it easy to change the size of the low-pass filter. More on filtering is covered under section 6.3.5. The second term "q→cal" was add so the user could specify which method to use for tracking the center of the diffraction pattern.

6.3.3 f3tensor(1,1,1,h,1,w)

Function f3tensor()[16] is located in file Filter-lib.c see–appendix A.3. It allocates memory for loading the raw data from "scan" into a 3-D array. Since our image is two dimensional I set the first pointer range, arguments one and two of f3tensor() to one. The next two arguments set the range for image height and the final two arguments set the range for image width.

6.3.4 rlft3(array2,spec,1,h,1,w,1)

Function rlft3() is located in file rlft3.c see–appendix A.4. The function rlft3() finds the DFT or inverse DFT using the Fast-Fourier-Transform algorithm. Its arguments are defined as follows:

1^{st} **argument, array2:** 3-D array containing data for which the DFT and inverse DFT are calculated. This argument is actually a 2-D array since its "depth" is set to one.

2^{nd} **argument, spec:** 2-D array containing data at critical frequency[17].

3^{rd} **argument, 1:** Specifies depth of image and in our case its one.

4^{th} **argument, h:** Specifies height of image.

5^{th} **argument, w:** Specifies width of image.

6^{th} **argument, 1:** "1" if DFT is found and "-1" if inverse DFT is found.

[16] Was taken from "NUMERICAL RECIPES in C"

[17] Used when "aliasing" is considered ; which is not the case here.

6.3.5 lowpass(array2,spec,fltr,w,h)

Function lowpass() is located in file Filter-lib.c see–appendix A.3. The definitions of "array2", "spec", "w", and "h" are the same as for function rlft3() defined above. The argument "fltr" specifies the size of the filter to apply. Essentially, lowpass() sets all frequency components greater than fltr/2 to zero. This acts to remove high-frequency noise but still maintain frequency components needed to reconstruct the image. For window size (256x256) the filter size is "28"[18].

6.3.6 fcentroid(array2,q,w,h,cen)

Function fcentroid() is located in file fcentroid.c see–appendix A.5. The function fcentroid() uses the centroid method for finding the absolute position of the diffraction pattern center and error in center. Arguments, "array2", "q", "w", and "h" have the same definitions as for functions filters() and rlft3(). The argument "cen[19]" is an array where calculated data are stored. The function "fcentroid()" does the following:

1. **Estimate center of diffraction pattern**
    - Pixel intensity levels are summed for each row and column. The row and column with maximum sum are used initially to estimate the center of the diffraction pattern. By doing this the actual window used to find the pattern center may be approximately centered over the diffraction pattern.
2. **Find Total Counts**
    - while determining the row and column with the peak pixel sum the total sum of all pixel intensities is found and saved in "cen[4]".
3. **Determine window size used to find centroid**

[18] Inspection of the DFT for upstream and downstream pinholes shows that frequency components greater than 14 were negligible in magnitude. This localization in the frequency-domain was further supported when analyzing the DFT of the (ideal diffraction patterns shown in figure-4). Therefore, frequency components greater than 14 were assumed to be caused by noise.

[19] Actually identical to argument "centroid" in function "filters()", just renamed when passed to "fcentroid"

- The edge that the estimated center of the diffraction pattern are closer to, the top, bottom, left or right is found. The edge closest to the diffraction-pattern-center forms one side of a square which surrounds the estimated center of the pattern. Thus, the window used to find the center of the diffraction pattern is smaller than the original-image-window[20] depending on how far off center the diffraction pattern peak is.

4. **Find Center of Diffraction Pattern**

   - The center and error in center of the diffraction pattern is found using equations 3 and 4. The X-position, Y-position, error in X-position, and error in Y-position is saved in "cen[0]", "cen[1]", "cen[2]", and "cen[3]".

6.4 System Setup and Operation

At the beginning of this report I mentioned that the type of camera and laser were predetermined. As a result, the only design choices were the size of pinhole and camera settings. Having chosen the pinhole size in section-4.1 and additional software in section-4.2; in this section I recommend various ways to setup and operate the laser, camera, and pinhole.

6.4.1 System Calibration

It was found that the centroid and phase-shift methods for finding the center of the diffraction predict similar results. The image can be offset[21], via the white-balance level, so only the central maximum of the diffraction pattern is visible (see figures 23 and 35). By doing this the diffraction pattern is completely confined within the picture window. As a result the correspondence between the two methods becomes almost identical. In the following procedures the laser and camera are tuned so only the central maximum of the diffraction pattern is visible. While testing it was found that the peak intensity

[20] Note the "original-window" is the one containing all data passed from function "filters()". The "actual-window" is the one centered about the estimated diffraction pattern center and is reduced in size. The value of doing this is if less than half of the diffraction pattern is in the original window; a reasonable estimate of its center is still possible without weighing one side of the pattern more heavily than the other.

[21] When I say offset Its meant that a fixed intensity level is subtracted from the entire image.

level of a picture is largest when the transferscale is set to four. Therefore, initially the brightness level is set to zero and the laser intensity increased to produce an image with maximum gray-scale levels. Once the best laser intensity is found than the transfercale may be decreased, and the appropriate brightness levels found. With the software developed so far, I reccomend the following procedures for laser, pinhole, and CCD-camera setup.

1. Alignment of laser and pinhole
   - Align laser so diffraction pattern is centered in the camera window.
   - Insure the pinhole is positioned in X-Y plane see figure-1.
   - Fix laser and camera alignment so they can be used as a valid reference.
2. Laser Intensity
   - Laser Intensity may be controlled by coupling two polarizing filters to the beam expander.
   - The following camera settings are recommended:
     (a) Filter → -F 28
     (b) Calibrate mode → -C 1
     (c) White-balance→ -w 70.
     (d) Brightness→ -b 0.
     (e) Transferscale→ -s 4.
   - With the above camera settings adjust the laser, via polarizing filters, to give the peak gray-scale level at the camera.
   - If parts of the image are non-zero, other than the central maximum, than the "white-balance" level should be increased by and the laser readjusted in the way described in the previous point. If the white-balance level and laser are set properly only the central peak of the diffraction pattern will be non-zero.
   - Once laser intensity is fixed change transferscale to → -s 2 and increase brightness level to give peak gray-scale level. Record camera settings.
   - Change transferscale to → -s 1 and change brightness level to give peak gray-scale level.

- Again, record camera settings.

3. Using largest window size and appropriate camera settings; take a picture to find the X and Y coordinates of the pinhole center.
4. Once the "absolute" coordinates of the pinhole are found set calibrate mode to $\rightarrow$ -C 0. This toggles tracking of the pinhole from the centroid-method to the phaseshift-method, see section-2 .
5. From this point on the time between pictures and size of picture are determined by "TCL".. If window size is changed between pictures the camera settings found above should be used.

6.4.2 System Operation

When the laser, camera, and pinhole are installed on the E614 detector there are two factors which can be change at any time:

1. **Time between pictures**
2. **Choice of Camera settings**

The above factors are related since the minimum time between pictures is limited by the choice of camera settings. For example, a picture size of (240x320) pixels will take longer to transfer from the CCD-camera to computer and longer to perform calculations than a picture of size (60x80) pixels. This is logical since at every step you deal with sixteen times more data with the (240x320) picture compared with the (60x80) picture. To minimize time between pictures the following recommendations are made:

1. **Use phase-shift method for finding the center of the diffraction pattern.**
   - The phase-shift method requires less computations than the centroid method. For example, to find the center of the diffraction pattern the following steps are needed.
     - Finding DFT of picture.
     - Read (0,1) and (1,0) terms of DFT to find phase.
   - Where the centroid method requires:

- Finding DFT of picture.
- Apply low pass filter.
- Find inverse DFT.
- Estimate center of diffraction pattern.
- Find actual center of diffraction pattern using equation-3.

2. **Choose smaller picture windows**

   - Smaller picture windows require less memory and are computationally quicker at all levels. The down side is resolution and/or the field of view is reduced.

The phase-shift method can be simplified further by finding the DFT for just the two frequencies of interest , (k_1=0,k_2=1) and (k_1=1,k_2=0), see equations 6 and 7 in section-2. By finding the phase directly for the two frequencies concerned; the FFT algorithm may be skipped. The total computations required to find the "real" and "imaginary" components for the two harmonics in question is reduced from $Nlog_2(N)$ computations to "N" computations. Where "N" is the total number of pixels. A comparison can be made between the phase-shift and centroid methods based on total computations required to estimate the center of the diffraction pattern and error in center. For this comparison the raw unfiltered[22] data is used with the centroid method. Table-4 summarizes total computations for the two methods. Its seen that the Phase-shift method is computationally simpler then the centroid-method, used with unfiltered data, and has the additional benefit of being insensitive to high frequency noise.

Type of Computation	Phase	Error in Phase	Centroid	Error in Centroid
Multiplication's	$4N_1N_2$	0	$2N_1N_2$	$2N_1N_2 + N_1 + N_2$
Additions	$4N_1N_2$	0	$4N_1N_2$	$2(N_1N_2 + 2N_1 + 2N_2)$

Table 4: The table above sumerizes the computations required to estimate the center of pinhole and error in center using the phase-shift and centroid methods. All estimates are based on equations 3, 4, 6, and 7 in section-2.

[22]The raw unfiltered data refers to the picture before any filtering is performed. Here, I suggest using the raw-data to see what the minimum number of computations are require to estimate the center of the pinhole using the centroid method

Total computations required for the phase-shift method are:

- Total multiplications=$4N_1N_2$
- Total additions=$4N_1N_2$

Total computations required for the centroid-method are:

- Total multiplications= $4N_1N_2 + N_1 + N_2$
- Total additions= $6N_1N_2 + 4(N_1 + N_2)$

Once the camera, pinhole and laser are mounted on the detector the choice of when pictures are taken is decided by "TCL". The actual speed with which successive picture may be taken still needs to be tested. Its been proposed that taking pictures quickly for some predetermined time might be useful for detecting vibrations[23]. While most of the time pictures would be taken at regular intervals of greater length. Once "TCL" is interfaced with the CCD-camera a timing schedule for when pictures should be taken may be worked out.

7 SYSTEM TESTING

7.1 General Approach

Testing consisted of taking pictures of the pinhole-diffraction-pattern for various locations of the pinhole. The computer code developed estimates the center of the diffraction pattern at the same time the picture is taken. All data such as the pinhole position, error in position, and total sum of all pixel intensities was written to a data file. For the case where the pinhole was moved in regular increments in one direction; all data for that run is written to a particular file. This procedure was repeated for the appropriate pinhole in both the upstream and downstream locations.

CCD-camera settings such as brightness-level[24] and white-balance[25] were set at the beginning of each run and left that way until the run

[23] One goal is to take pictures 120 times per second so 60 Hz vibrations could be detected.
[24] Brightness-level controls the exposure time of the picture.
[25] White-balance controls the offset of the image(e.g. subtracts a constant from the intensity level for each pixel

was finished. Both brightness-level and white-balance were set so the peak of the diffraction pattern was as large as possible but not exceeding the maximum allowable gray-scale level.

While testing, four types of diffraction patterns were studied:

The first was for the upstream pinhole located in the upstream position. The camera was set so the secondary peaks of the diffraction pattern were partially visible, see figures 15 and 16 in appendix-B, for the non-filtered and filtered versions. The respective cross-sections for these picture are located in figures 17 and 23 in appendix-B.

The second diffraction pattern was for the same pinhole in the same location as the first but with different "brightness-level" and "white-balance" settings. The CCD-camera was set so only the central maximum of the diffraction pattern was visible, see figures 21, 22 23 and 24 in appendix-B.

The third diffraction pattern was for the downstream pinhole located in the downstream position. Again the camera was set so the secondary peaks of the diffraction pattern were partially visible, see figures 27, 28, 29 and 30 in appendix-B.

The fourth diffraction pattern was for the downstream pinhole located in the downstream position. The camera was set so only the central maximum of the diffraction pattern was visible, see figures 33, 34, 35 and 36 in appendix-B.

The reason for studying diffraction patterns with only the central maximum visible is they are more localized in space. Thus, smaller picture sizes may be used to capture the diffraction pattern. As a result, pictures can be taken more quickly since less data is processed by the camera and computer. Therefore, if pictures are to be taken quickly the camera settings may be changed to localize the diffraction pattern. My objective was to compare the accuracy of the localized and non-localized diffraction patterns. If the accuracy is similar than the localized diffraction pattern would be used in the final system.

7.2 Effects of Filtering

The effects of filtering are seen in figures 16, 22, 28 and 34 in appendix-B. The respective non-filtered images are seen in figures

figures 15, 21, 27 and 33. We see the spots and vertical lines present in the non-filtered image are not present in the filtered image. To accomplish this all frequency components, of the Discrete Fourier Transform or DFT, greater than fourteen were made zero (see DFT X-sections in figures 19, 25, 31 and 37). Closer inspection of the DFT X-sections shows that the primary harmonics required to rebuild the image are within ten of the "zero", or "DC", frequency. Thus, removing harmonics greater than fourteen will have little effect on the main image. But, if high-frequency noise is present it will be removed. The advantages in filtering is the diffraction pattern its less sensitive to dust on the CCD-array, Laser and beam-expander. This makes the system more stable in a dusty environment.

7.3 Pinhole Tracking

The pinhole was moved in regular increments of 20 ± 1 μm in one direction. In each new position a picture was taken and the center of the diffraction pattern found. Plots were made comparing the actual position of the pinhole with the position calculated using the CCD-camera. A plot of the upstream and downstream tracks, for the offset diffraction patterns, is shown in figure-10.

The purpose of figure-10 is to show the relation between moving the pinhole and detecting movement is "reasonably" linear. The "offset" diffraction patterns were used since both centroid and phase-shift methods for estimating the center of the pinhole produce the same slope. As a result, the figure was simplified since only two slopes were needed instead of four. Each pixel is approximately 10 μm by 10 μm in size. The detected change in position of the pinhole was found in units of pixels and than converted to "μm" by multiplying by ten. Therefore, if the position of pinhole is actually change by 20 μm then we expect the detected change in position also to be 20 μm. It follows that both the "upstream" and "downstream" slopes should equal one with the scaling used. However, we see from figure-10 that the average upstream or downstream slopes are "1.27" and "1.73", respectively. I believe the deviation from expected is explained by the divergence of the laser. Laser divergence was measured to be 6.5 mrad. Using geometry, its easy to find how much the average trajectory of light changes when the pinhole position is changed. Thus, the camera will see the actual shift in

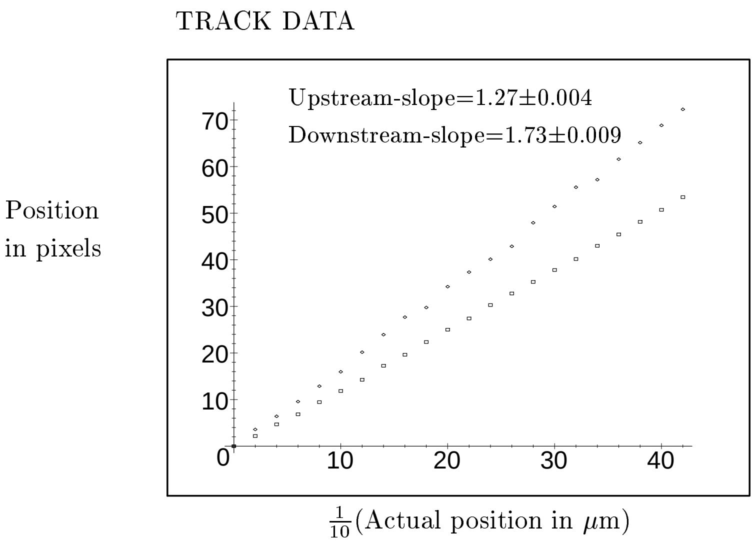

Figure 10: Both upstream and downstream pinholes were moved in increments 20±1 μm along the X-axis (see figure-3). Actual displacement is along the X-axis and measured displacement along the Y-axis. The "offset" diffraction patterns were used to calculated the center of both pinholes. The slopes and associated errors were found using "least-square" analysis. The "box-pattern" equals the upstream pinhole and the "diamond-pattern" equals the downstream pinhole. Laser wavelength, λ=670 nm.

position of the pinhole along with an additional shift caused by the change in direction of the diverging light. Using the geometry of figure-3 the expected slopes were found to be:

Upstream slope $= 1.21$

downstream slope $= 1.68$

We see theres good aggreement between the actual slopes and the observed slopes; justifying my explanation.

For general reference track data for all diffraction patterns tested are found in figures 20, 26, 32 and 38. For these figures both the X and Y coordinates of the pinhole are tracked using both the phase-shift and centroid methods.

7.4 Scatter

Figures 11,12,13 and 14 were found by subtracting the average slope of the track data from the actual track data. For all these figures the centroid and phase-shift methods for estimating the center of the pinhole are compared.

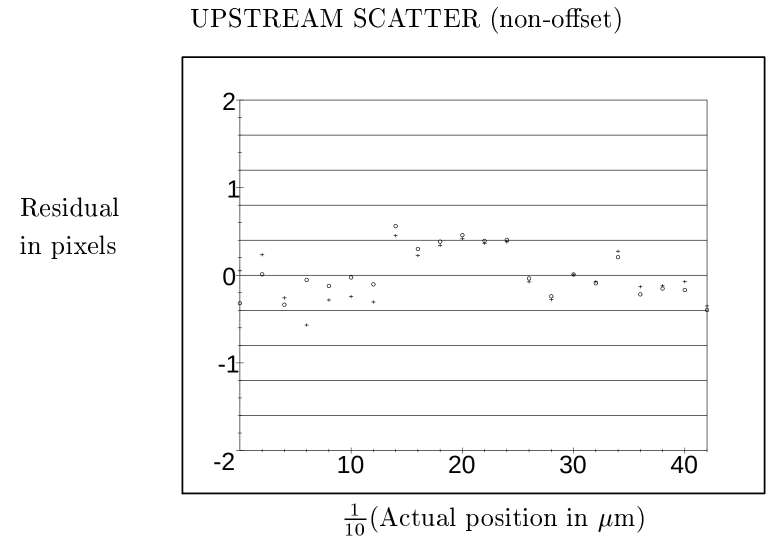

Figure 11: The upstream pinhole is moved in increments 20$\pm$1 μm along the X-axis of the apparatus(see figure-3). The "Residual", plotted along the y-axis in the figure above, is found by subtracting the average slope of the track data from the actual track data. The "non-offset" diffraction pattern was used when calculating the center of pinhole. The "cross-pattern" equals data found using centroid method and the "diamond-pattern" equals data found using phase-shift method. Laser wavelength, λ=670 nm.

Looking closely at figures 11 and 12 we see that the scatter of the data is confined with $\pm$0.4 pixels or 4 μm. In fact, the standard deviation of the scatter for the non-offset and off-set cases is (0.30 and 0.24) pixels respectively. Thus, a reasonable estimate of error would be $\pm$ 0.4 μm. For comparison the average error predicted from equations 4 and 7 for the respective phase-shift and centroid methods are summarize below:

- **Non-Offset case**
  - Error in X-phase = 0.06 pixels
  - Error in X-centroid = 0.07 pixels
- **Offset case**
  - Error in X-phase = 0.06 pixels

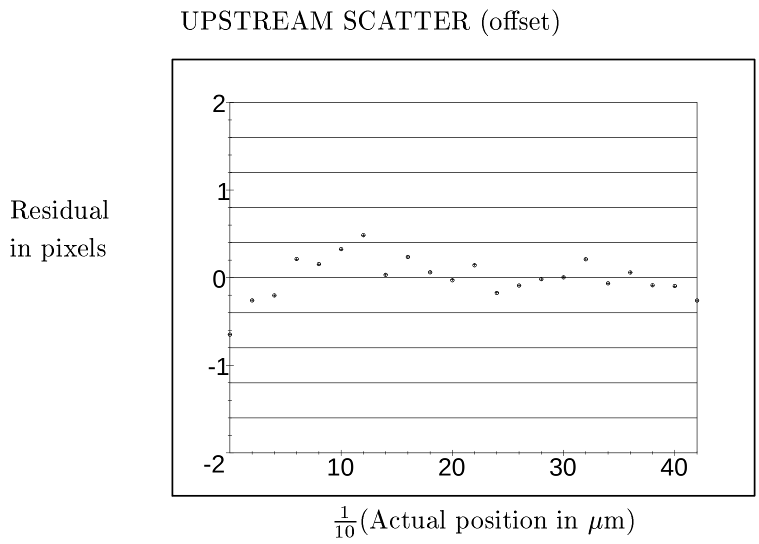

Figure 12: The upstream pinhole is moved in increments 20±1 μm along the X-axis of the apparatus(see figure-3). The "Residual", plotted along the y-axis in the figure above, is found by subtracting the average slope of the track data from the actual track data. The "offset" diffraction pattern was used when calculating the center of pinhole. The "cross-pattern" equals data found using centroid method and the "diamond-pattern" equals data found using phase-shift method. Laser wavelength, λ=670 nm.

– Error in X-centroid = 0.08 pixels

We see there is a significant difference between the error observed compared to what was calculated. I expect vibrations of the equipment are responsible, in part, for these differences. Another observation is that for "non-offset" scatter, figures 11 and 13, the phase-shift and centroid method do not correspond. But for the "offset" scatter, in figures 12 and 13, the correspondence is excellent. I expect the reasone for the difference is the "offset" diffraction pattern, see figure-24 in appendix-B, is completely confined within the picture window (i.e. pixels of intensity zero surround the diffraction pattern). For this reason, when the pinhole and corresponding diffraction pattern is moved a small amount the diffraction pattern is still completely confined within the picture window. Where for the "non-offset" diffraction pattern, see figure-18 in appendix B, a small shift in pinhole position will slide non-zero elements of the diffraction pattern off the screen. Creating a dependency between the diffraction pattern and pinhole position. Effecting the tracking between the phase-shift and centroid methods.

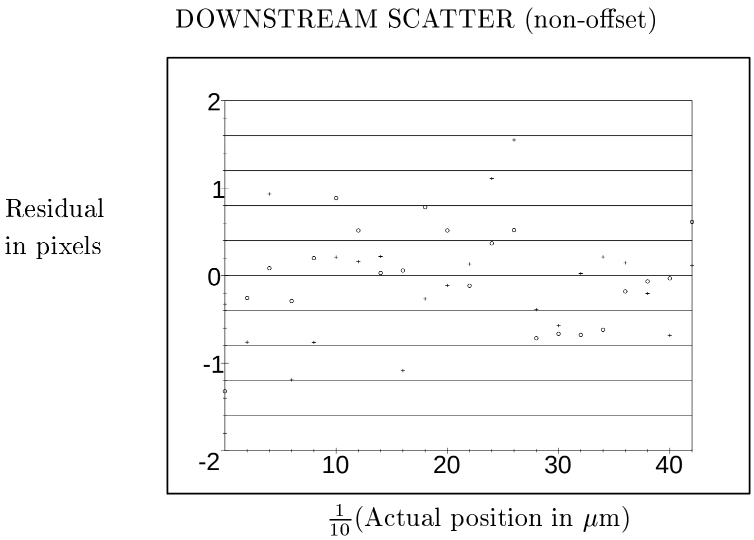

Figure 13: The downstream pinhole is moved in increments 20±1 μm along the X-axis of the apparatus(see figure-3). The "Residual", plotted along the y-axis in the figure above, is found by subtracting the average slope of the track data from the actual track data. The "non-offset" diffraction pattern was used when calculating the center of pinhole. The "cross-pattern" equals data found using centroid method and the "diamond-pattern" equals data found using phase-shift method. Laser wavelength, λ=670 nm.

Scattering for the downstream pinhole, see figures 13 and 14 is similar to the upstream pinhole except for the following main difference. The scattering of data is larger than for the upstream case. The standard deviation for both phase-shift and centroid methods is (0.55 and 0.67)-pixels respectively for figure-13 ; and (0.59 and 0.59) respectively for figure-14. Again, for comparison, the average error predicted by equations 4 and 7 for the respective phase-shift and centroid methods are summarize below:

- **Non-Offset case**
  - Error in X-phase = 0.04 pixels
  - Error in X-centroid = 0.03 pixels
- **Offset case**

- Error in X-phase = 0.04 pixels
- Error in X-centroid = 0.04 pixels

One factor wich may be responcible for the larger scatter is the divergence of the laser. Meaning, if the pinhole actually moves randomly with respect to laser than this motion will appear larger for the downstream pinhole than the upstream one. The reasoning would follow directly from the discussion on the effects of a divergent laser beam on tracking of the pinhole(see figure-10). Diverging light will cause movement of the pinhole to be amplified; the further the pinhole is from the camera (see section-5.3). Another factor that might cause larger scatter for the downstream pinhole is random rotations of the laser. Minor rotations of the laser will change the trajectory of the light passing through and cause additional variation. This effect would be more noticeable for the downstream case than the upstream case because the light passing through the downstream pinhole has more distance to diverge than for the upstream pinhole.

8 DATA ANALYSIS

Looking over the data collected its clear that the position of the pinhole can be estimated to within an accuracy of ± 4 μm for the upstream pinhole and ± 7 μm for the downstream pinhole. As explained earlier a possible difference in accuracy between the upstream and downstream pinholes is due to the divergence of the laser beam and/or minor rotations of the laser. It seem natural that these two effects are partly responsible for what's observed; because both will increase the error in the estimated position of downstream pinhole more than in the upstream pinhole (which was observed). Both these effects will increase the observed error in pinhole position. As a result, the difference between the observed error and calculated error may also be do to pinhole movement or random rotations of the laser.

However, the estimated error in pinhole position is based strictly on the image captured by the picture. It does not reflect possible variation of the laser beam as function of time[26] and/or space. Testing in a vibration free environment would separate what portion of

[26]The intensity of the laser beam X-section may vary as a function time and/or space

DOWNSTREAM SCATTER (offset)

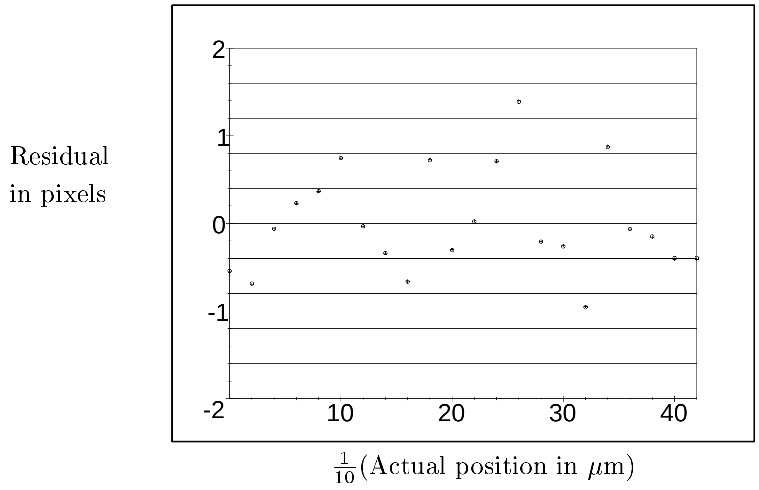

Figure 14: The downstream pinhole is moved in increments 20±1 μm along the X-axis of the apparatus(see figure-3). The "Residual", plotted along the y-axis in the figure above, is found by subtracting the average slope of the track data from the actual track data. The "offset" diffraction pattern was used when calculating the center of pinhole. The "cross-pattern"= data found using centroid method and the "diamond-pattern"= data found using phase-shift method. Laser wavelength, λ=670 nm.

error is caused by random movement of the pinhole and laser from the portion caused by variations of the laser beam intensity and CCD-camera-response.

Its observed, in figures 12 and 14, that the centroid and phase-shift methods for estimating the center of the pinhole are almost identical. These figures correspond to the "offset" diffraction pattern. I recommend using the "offset" over "non-offset" diffraction patterns for the following three reasons:

- The "offset" diffraction pattern is more localized than the "non-offset" one. Allowing smaller pictures to be taken, with the same resolution, while still capturing the entire diffraction pattern. As a result pictures may be taken more quickly since the size of the pictures in bytes is smaller.

- The phase-shift and centroid methods produce almost identical results (see figures 12 and 14). Allowing the phase-shift method

,which is computationally quicker, to be used.

- Permits using diffraction patterns with even narrower central maximum see figure-5. The distortion created by using larger pinholes wouldn't matter since only the upper part of the central peak is used.

Therfore, pinholes larger than the ones tested might be preferred. The central maximum will be narrower allowing use of smaller picture windows. Any distortion which results can be offset by the appropriate white-balance level. Another advantage to the "offset" diffraction pattern is there's little worry of driving part of the diffraction pattern off the picture window. As a result there will be a region within the picture window where the detected diffraction pattern is completely confined within the picture window. Any movement of the pinhole outside of this region would introduce errors because part of the diffraction pattern is off the picture window. To see this consider figure-18. The width of this diffraction pattern is approximately 100 pixels. For a window of size 240 by 320 pixels the pinhole could move 700 μm vertically or 1100 μm horizontally from the center of the window before the diffraction pattern starts to slide of the edge of the picture. Thus, the region where the diffraction pattern is completely confined within the picture window is 700 μm by 1100 μm. If we expect the detector to move more than this than a narrower diffraction pattern could be used. In the final system and "out of bound" flag could be added to TCL warning if the pinhole starts to move beyond the acceptable operating range.

9 FUTURE WORK

Eventually, multiple alignment monitoring systems will be placed on the E614 detector. Before the point of installation a final system design is required. Although, much work has been done to prove the viability of this system; further testing and design is required. The following, is a list of future work in approximate chronological order:

1. **Repeat testing with mirrors instead of pinholes**.
   - It was mentioned at the collaboration meeting, of August 20, 1999, that a system where the laser and camera are

mounted on the same end of the detector would have advantages. One advantage is both laser and camera may be mounted on the fixed end of the detector. Which is unaffected by dismantling of the detector for maintenance. To allow placing both laser and CCD-camera on the same end of the detector; it was proposed that a mirror of similar size to the pinholes tested be mounted in the detector instead of the pinholes.

- Mirrors of appropriate sizes will need to be built.
- Similar tests performed with the pinhole will need to be repeated for the mirror.

2. **Perform tests in a non-vibration environment.**
   - As discussed in section-6, the error in the pinhole-position is likely due to actual movement of the pinhole and laser. Repeating tests on an optical bench would determine exactly how accurately the system can detect movements of the pinhole.
3. **Perform tests over long time scales**
   - Measurements should be taken in regular interval to simulate actual operation. Perhaps conduct test over a number of weeks.
4. **Find why vertical lines were noticed in pictures**
   - Vertical lines were noticed in all pictures. The cause of these were not found but it may be related to the camera, laser, or polarizing filters on the beam expander.
5. **Interface with "TCL"**
   - "TCL" or Tool Command Language will send commands to the camera instructing it to take a picture. When a picture is taken the camera's source code will find the center of the pinhole, error in center, and total sum of all pixel intensities. "TCL" would read the calculated data, time stamp it, and record it for future reference. TCL may also produce a plot of pinhole-position as a function of time and display a picture of the pinhole.

6. **Optimize Computer Code**
   - The computer code needs to be optimized. While writing this report some redundancies were noted. In addition, if the "off-set" diffraction pattern is used the centroid method for calculating the position of the pinhole can be simplified. The steps for estimating the center of the diffraction pattern and sizing a symmetric window[27] around it could be dropped since the entire diffraction pattern will be confined within the picture window.
7. **Make Instructions for initial calibration**
   - In the final system the instructions required to find the initial CCD-camera and laser settings, similar to section-4.4.1, will need to be written up.
8. **Develop final Mechanical design**
   - Brackets need to be fitted to the CCD-camera and laser to allow mounting on the detector.
   - A method to align the laser is required.
   - The final mirror design will need to be fitted to detector and secured.
9. **Make Instructions for installation of system on detector**

10 CONCLUSION

The ability of a CCD-camera, pinhole, and laser to monitor alignment of the E614-detector was studied. Computer code was added to the CCD-camera's source code to calculate the center of pinhole and its error in position. In this way, when a picture is taken, all calculated values are found at the same time.

Two methods were developed to estimate the center of the pinhole:

[27]The centroid method is described in section-4.3.6. It turns out that the diffraction patterns will distort by filtering if it slides off the picture window. This is caused by a "step-function" multiplying the diffraction pattern. As a result, additional high-frequency harmonics are needed to rebuild the image. When the lowpass filter is applied these harmonics are thrown out causing distortion.

- The first method, called the centroid method, was to take the Discrete-Fourier-Transform or DFT of a picture, apply a low-pass filter, find the Inverse Discrete-Fourier-Transform and finally calculate the centroid of the resulting image. Filtering had the benefit of removing high frequency noise such as dust spots on the camera.
- The second method, called the phase-shift method, was to find the first vertical and horizontal harmonics of the Discrete-Fourier-Transform. The change in phase of these harmonics corresponds to the change in position of the center of the pinhole.

Its recommended that the first method be used to estimate the initial position of the pinhole and the second method be used to track its position afterwards. The two methods above produce almost identical results as long as the camera settings were such that the diffraction pattern detected by the CCD-camera was completely confined within the picture. In addition, to minimize error, the CCD-camera and laser intensity were set so the diffraction pattern detected had peak intensity as close as possible to the maximum gray-scale level of the camera.

The pinhole radii tested were "0.495" mm and "0.755" mm for the respective upstream and downstream ends of the detector stack. However, final analysis of the data collected suggests there's little disadvantage to using larger pinholes with the methods developed for estimating the center of the pinhole. The advantage of larger pinholes is the central peak of the diffraction pattern is narrower. Permitting smaller pictures to be taken that are quicker to process. Testing with larger pinholes is required.

The accuracy with which the upstream and downstream pinholes were detected was ± 4 μm and ± 7 μm respectivally[28]. However, its possible that some of this error was actually due to random movements of the CCD-camera, or laser. To distinguish between error in the pinhole position and actual movement of the pinhole or laser I would recommend additional testing on an optical bench.

Future work will involve moving the CCD-camera and laser to the same end of the detector and replacing the pinholes with mirrors of

[28]The above accuracy's were based on testing with the equipment described and methods developed for estimating the center of the pinhole.

similar size. This method would work in a similar fashion as with the pinholes, but allows mounting the laser and CCD-camera on the fixed end of the detector. By doing this the camera and laser alignment is unaffected by dismantling of the detector. Eventually, multiple systems will be interfaced with Tool-Command-Language or "TCL". "TCL" will decide when pictures should be taken and how often. Finally a mechanical design for the installation of the laser, pinhole/mirror, and CCD-camera must be developed.

In conclusion the laser, pinhole, and CCD-camera system has been proven to be an accurate way to monitor position. Its clear, the methods developed can be extended to multiple laser and CCD-camera systems mounted on the E614 detector. Enabling an accurate way to monitor various positions of the detector stack in the plane perpendicular to beam line.

APPENDIX

A SOFTWARE

A.1 qcam.c

A.2 filter.c

A.3 Filter-lib.c

A.4 rlft3.c

A.5 fcentroid.c

B FIGURES

B.1 Figures for Upstream Pinhole (non-offset)

UPSTREAM DIFFRACTION PATTERN

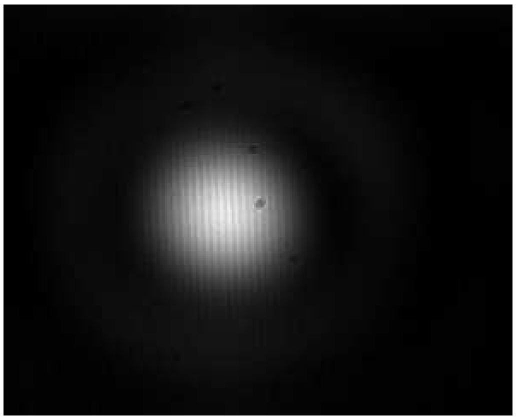

Figure 15: The figure above is a picture of the non-filtered diffraction pattern. The size of the picture is 240-pixels by 320-pixels. The axes follow the same orientation as in figure-3. Camera settings are: -b 75 -w 94 -s 1. The pinhole position and radius are, z_{up}=88 cm and a_{up}=0.495 mm, respectivally (see figure-3). Laser wavelength, λ, equals 670 nm.

FILTERED UPSTREAM DIFFRACTION PATTERN

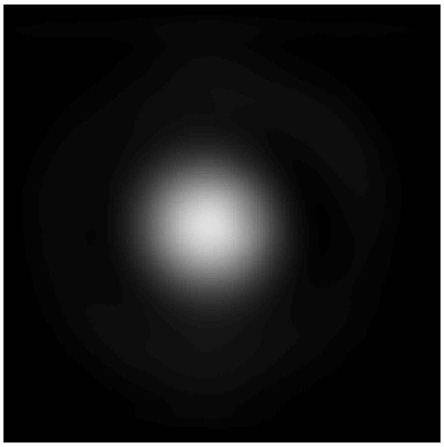

Figure 16: The figure above is a picture of the filtered diffraction pattern. The size of the picture is 256-pixels by 256-pixels. The axes follow the same orientation as in figure-3. Camera settings are: -b 75 -w 94 -s 1 -F 28 -C 1. The pinhole position and radius are, z_{up}=88 cm and a_{up}=0.495 mm, respectivally (see figure-3. Laser wavelength, λ, equals 670 nm.

UPSTREAM DIFFRACTION PATTERN

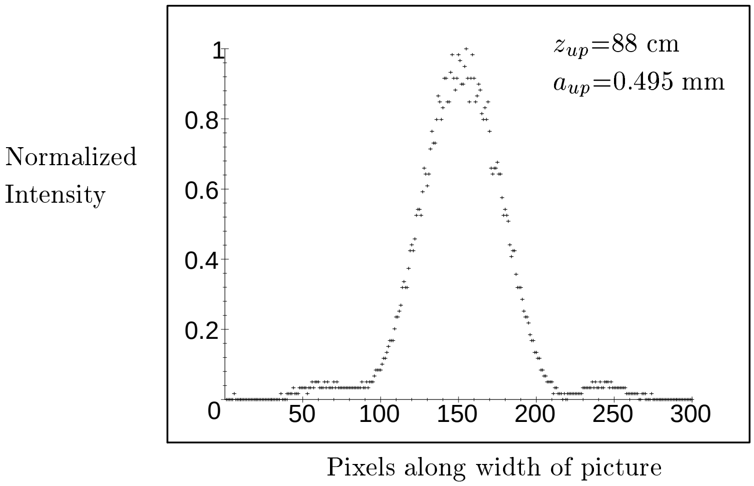

Figure 17: The "cross" pattern is the non-filtered diffraction pattern X-section. camera settings: -b 75 -w 94 -s 1 -F 28 -C 1. z_{up}=upstream pinhole position and a_{up}=upstream pinhole radius, see figure-1. Laser wavelength λ=670 nm.

FILTERED UPSTREAM DIFFRACTION PATTERN

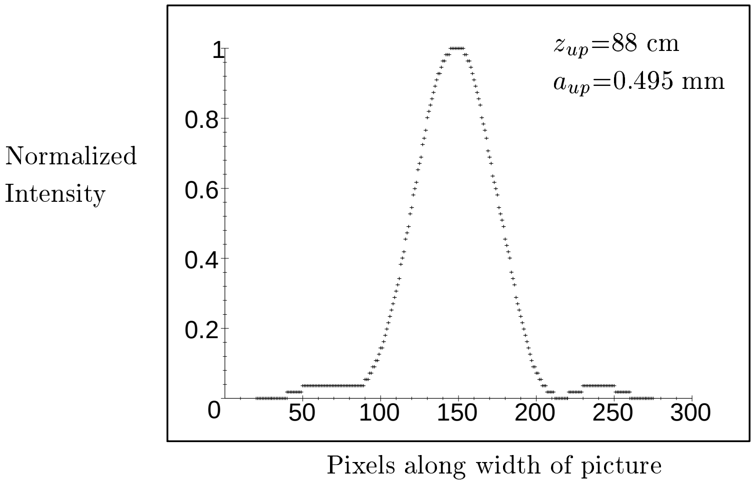

Figure 18: The "cross" pattern is the filtered diffraction pattern X-section. camera settings: -b 75 -w 94 -s 1 -F 28 -C 1. z_{up}=upstream pinhole position and a_{up}=upstream pinhole radius, see figure-1. Laser wavelength λ=670 nm.

DISCRETE FOURIER TRANSFORM

Normalized Magnitude

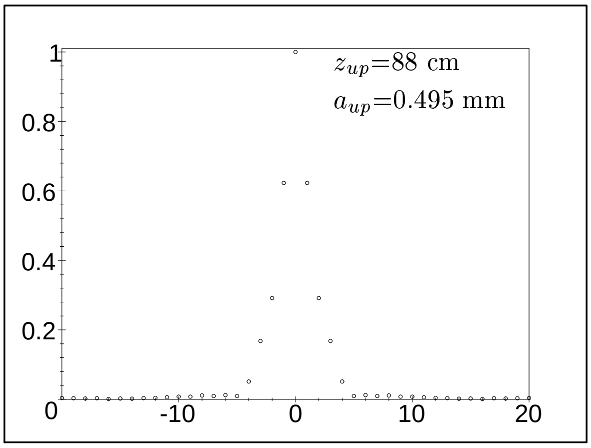

Pixels along width of picture

Figure 19: The "cross" pattern is the Discrete Fourier Transform X-section. camera settings: -b 75 -w 94 -s 1 -F 28 -C 1. z_{up}=upstream pinhole position and a_{up}=upstream pinhole radius, see figure-1. Laser wavelength λ=670 nm.

TRACKING PINHOLE POSITION

Position in Pixels

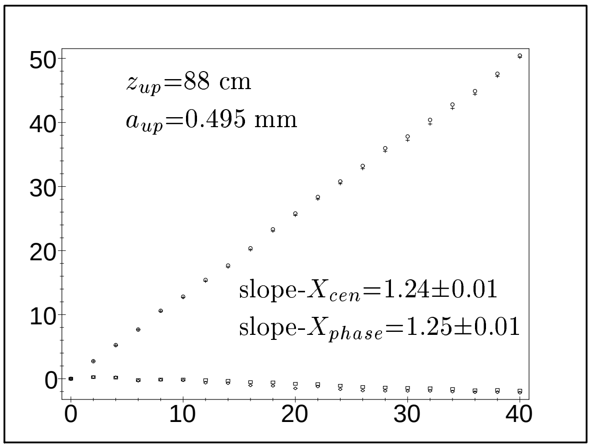

0.1x(Position in μm)

Figure 20: Pinhole moved in increments 20±1 μm along X-axis of the apparatus. Actual displacement is along the X-axis, of the figure above, and measured displacement along the Y-axis. Camera settings: -b 75 -w 94 -s 1 -F 28 -C 1. z_{up}=upstream pinhole position and a_{up}=upstream pinhole radius, see figure-1. Laser wavelength λ=670 nm. "cross-pattern"= X-position of centroid, "circle-pattern"= Phase-shift of first harmonic in X-direction, "box-pattern"= Y-position of centroid, "diamond-pattern"= Phase-shift of first harmonic in Y-direction.

B.2 Figures for Upstream Pinhole (offset)

UPSTREAM DIFFRACTION PATTERN

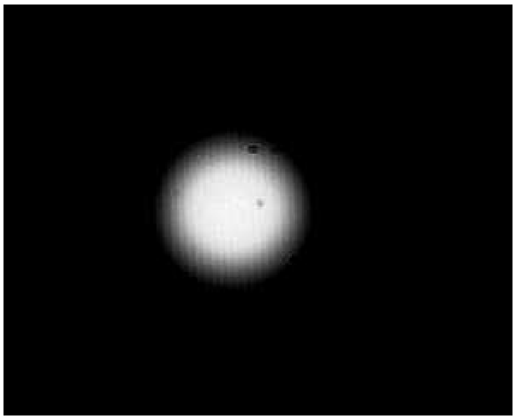

Figure 21: The figure above is a picture of the non-filtered, "offset", diffraction pattern. The size of the picture is 240-pixels by 320-pixels. The axes follow the same orientation as in figure-3. Camera settings are: -b 75 -w 94 -s 1. The pinhole position and radius are, z_{up}=88 cm and a_{up}=0.495 mm, respectivally (see figure-3). Laser wavelength, λ, equals 670 nm.

FILTERED UPSTREAM DIFFRACTION PATTERN

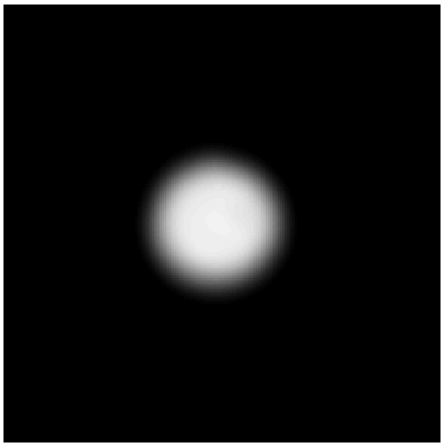

Figure 22: The figure above is a picture of the filtered, "offset", diffraction pattern. The size of the picture is 256-pixels by 256-pixels. The axes follow the same orientation as in figure-3. Camera settings are: -b 75 -w 94 -s 1 -F 28 -C 1. The pinhole position and radius are, z_{up}=88 cm and a_{up}=0.495 mm, respectivally (see figure-3. Laser wavelength, λ, equals 670 nm.

UPSTREAM DIFFRACTION PATTERN

Normalized
Intensity

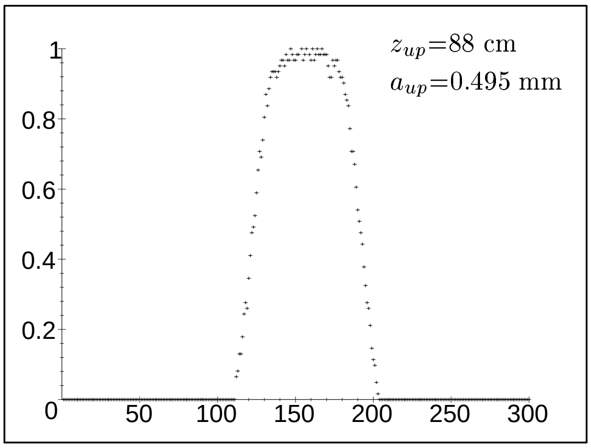

Pixels along width of picture

Figure 23: The "cross" pattern is the non-filtered diffraction pattern X-section. camera settings: -b 70 -w 100 -s 1 -F 28 -C 1. z_{up}=upstream pinhole position and a_{up}=upstream pinhole radius, see figure-1. Laser wavelength λ=670 nm.

FILTERED UPSTREAM DIFFRACTION PATTERN

Normalized
Intensity

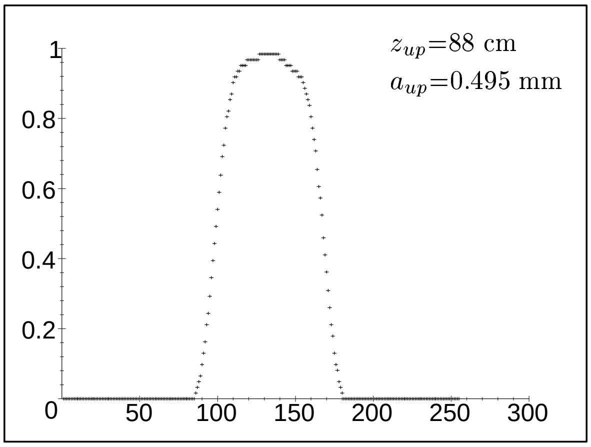

Pixels along width of picture

Figure 24: The "cross" pattern is the filtered diffraction pattern X-section. camera settings: -b 100 -w 70 -s 1 -F 28 -C 1. z_{up}=upstream pinhole position and a_{up}=upstream pinhole radius, see figure-1. Laser wavelength λ=670 nm.

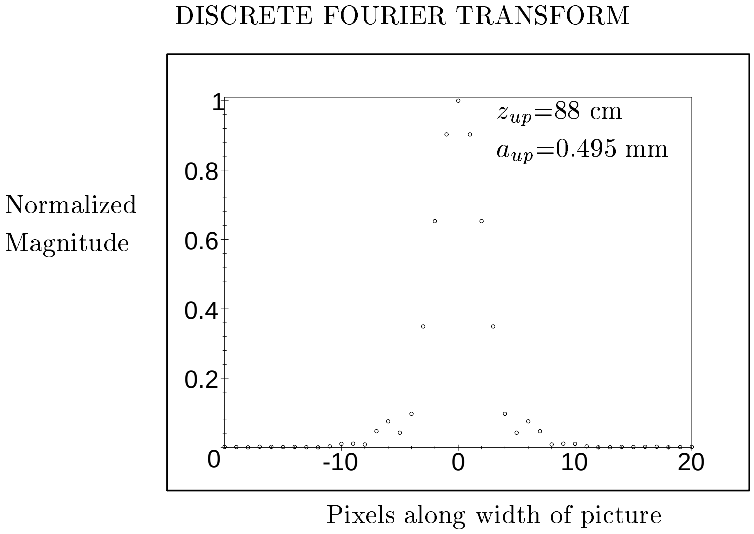

Figure 25: The "cross" pattern is the Discrete Fourier Transform X-section. camera settings: -b 100 -w 70 -s 1 -F 28 -C 1. z_{up}=upstream pinhole position and a_{up}=upstream pinhole radius, see figure-1. Laser wavelength λ=670 nm.

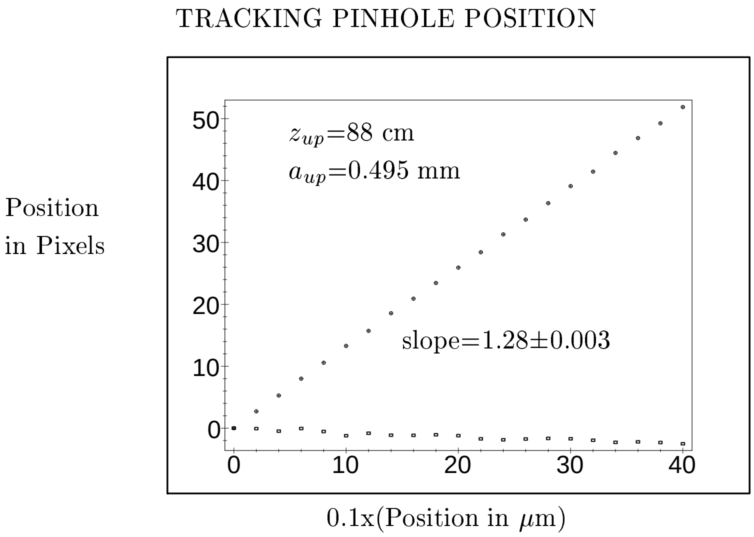

Figure 26: Pinhole moved in increments 20±1 μm along X-axis of the apparatus. Actual displacement is along the X-axis, of the figure above, and measured displacement along the Y-axis. Camera settings: -b 100 -w 75 -s 1 -F 28 -C 1. z_{up}=upstream pinhole position and a_{up}=upstream pinhole radius, see figure-1. Laser wavelength λ=670 nm. "cross-pattern"= X-position of centroid, "circle-pattern"= Phase-shift of first harmonic in X-direction, "box-pattern"= Y-position of centroid, "diamond-pattern"= Phase-shift of first harmonic in Y-direction.

B.3 Figures for Downstream Pinhole (non-offset)

DOWNSTREAM DIFFRACTION PATTERN

Y↑

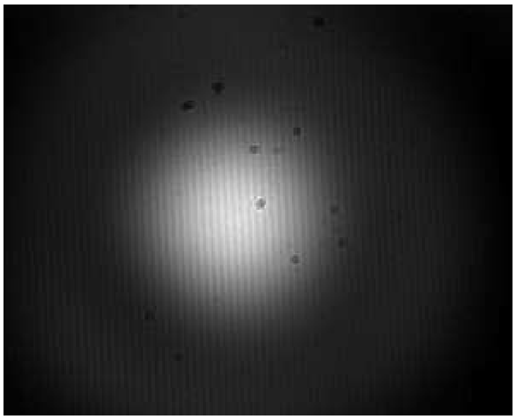

←X

Figure 27: The figure above is a picture of the non-filtered diffraction pattern. The size of the picture is 240-pixels by 320-pixels. The axes follow the same orientation as in figure-3. Camera settings are: -b 75 -w 94 -s 1. The pinhole position and radius are, z_{down}=208 cm and a_{down}=0.755 mm, respectivally (see figure-3). Laser wavelength, λ, equals 670 nm.

FILTERED DOWNSTREAM DIFFRACTION PATTERN

Y↑

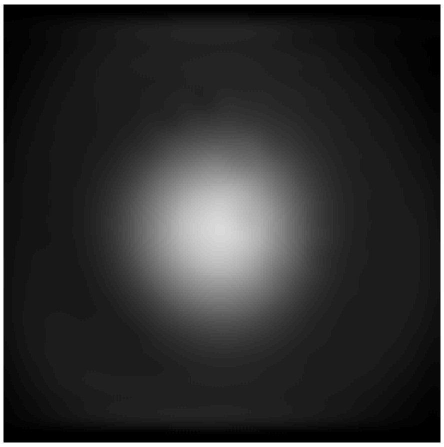

←X

Figure 28: The figure above is a picture of the filtered diffraction pattern. The size of the picture is 256-pixels by 256-pixels. The axes follow the same orientation as in figure-3. Camera settings are: -b 75 -w 94 -s 1 -F 28 -C 1. The pinhole position and radius are, z_{down}=208 cm and a_{down}=0.755 mm, respectivally (see figure-3. Laser wavelength, λ, equals 670 nm.

DOWNSTREAM DIFFRACTION PATTERN

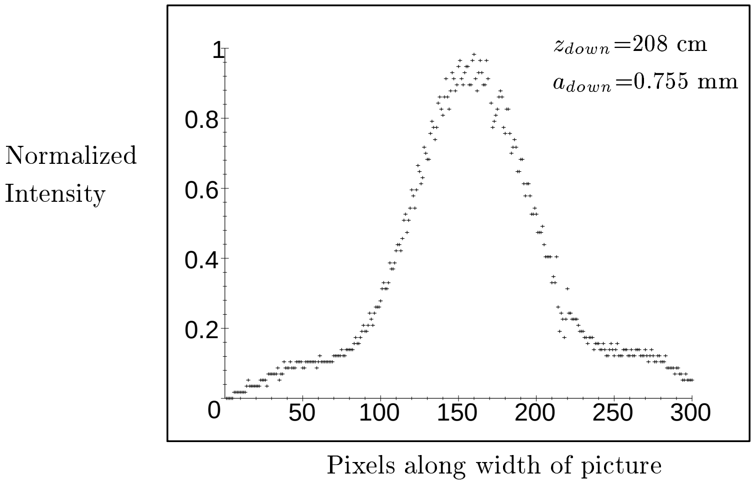

Figure 29: The "cross" pattern is the non-filtered diffraction pattern X-section. camera settings: -b 75 -w 94 -s 1 -F 28 -C 1. z_{down}= downstream pinhole position and $a_{downstream}$= downstream pinhole radius, see figure-1. Laser wavelength λ=670 nm.

FILTERED DOWNSTREAM DIFFRACTION PATTERN

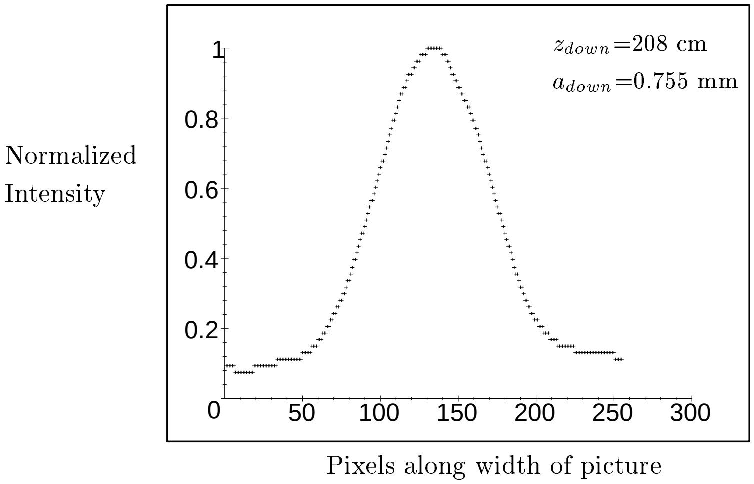

Figure 30: The "cross" pattern is the filtered diffraction pattern X-section. camera settings: -b 75 -w 94 -s 1 -F 28 -C 1. z_{down}=downstream pinhole position and a_{down}=downstream pinhole radius, see figure-1. Laser wavelength λ=670 nm.

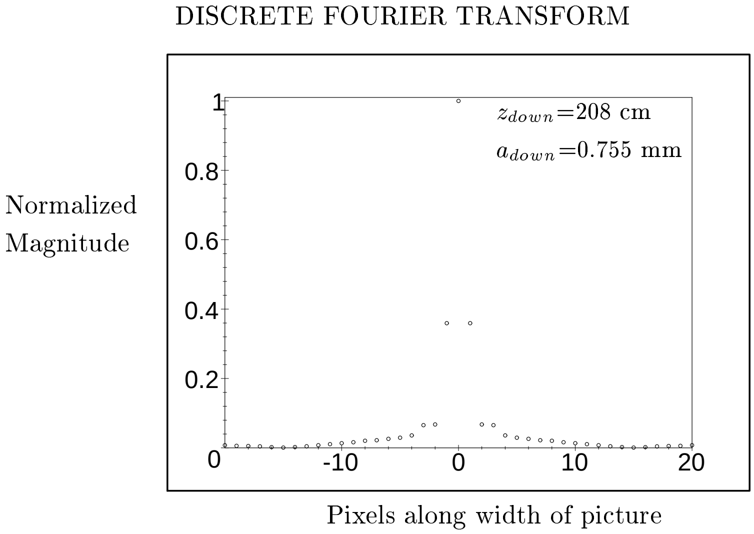

Figure 31: The "cross" pattern is the Discrete Fourier Transform X-section. camera settings: -b 75 -w 94 -s 1 -F 28 -C 1. z_{down}=downstream pinhole position and a_{down}=downstream pinhole radius, see figure-1. Laser wavelength λ=670 nm.

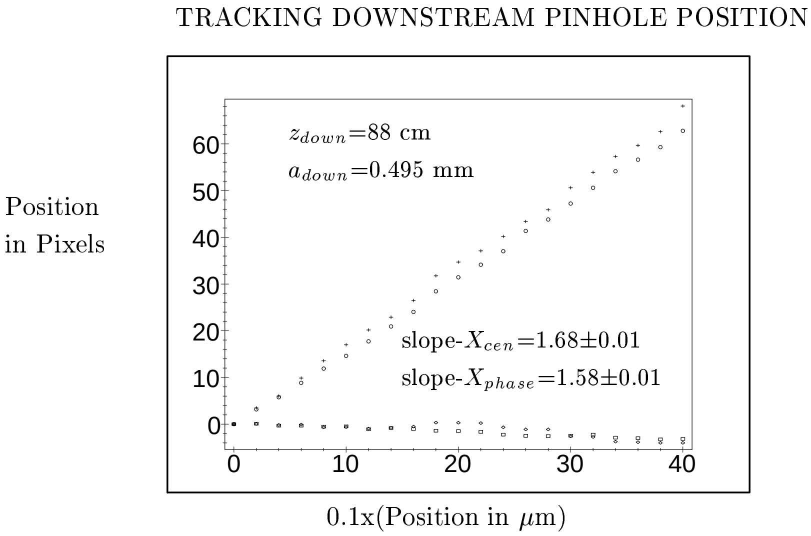

Figure 32: Pinhole moved in increments 20±1 μm along X-axis of the apparatus. Actual displacement is along the X-axis, in the figure above, and measured displacement along the Y-axis. Camera settings: -b 75 -w 94 -s 1 -F 28 -C 1. z_{down}=downstream pinhole position and a_{down}=downstream pinhole radius, see figure-1. Laser wavelength λ=670 nm. "cross-pattern"= X-position of centroid, "circle-pattern"= Phase-shift of first harmonic in X-direction, "box-pattern"= Y-position of centroid, "diamond-pattern"= Phase-shift of first harmonic in Y-direction.

B.4 Figures for Downstream Pinhole (offset)

DOWNSTREAM DIFFRACTION PATTERN

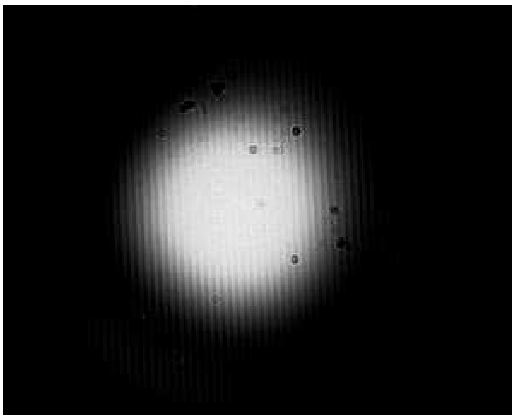

Y↑

←X

Figure 33: The figure above is a picture of the non-filtered "offset" diffraction pattern. The size of the picture is 240-pixels by 320-pixels. The axes follow the same orientation as in figure-3. Camera settings are: -b 75 -w 94 -s 1. The pinhole position and radius are, z_{down}=208 cm and a_{down}=0.755 mm, respectivally (see figure-3). Laser wavelength, λ, equals 670 nm.

FILTERED DOWNSTREAM DIFFRACTION PATTERN

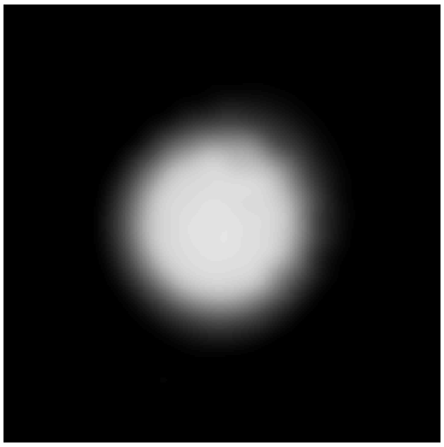

Y↑

←X

Figure 34: The figure above is a picture of the filtered "offset" diffraction pattern. The size of the picture is 256-pixels by 256-pixels. The axes follow the same orientation as in figure-3. Camera settings are: -b 75 -w 94 -s 1 -F 28 -C 1. The pinhole position and radius are, z_{down}=208 cm and a_{down}=0.755 mm, respectively (see figure-3. Laser wavelength, λ, equals 670 nm.

DOWNSTREAM DIFFRACTION PATTERN

Normalized Intensity

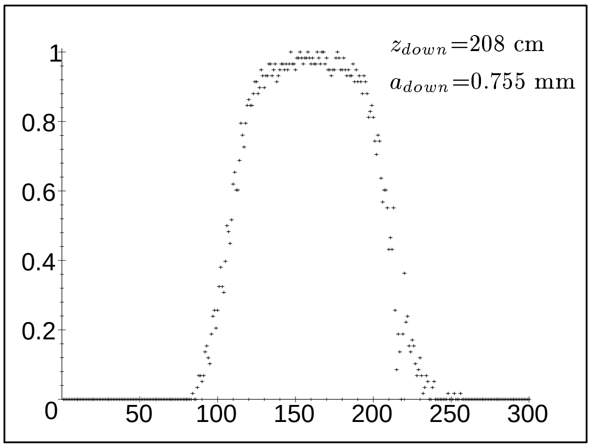

Pixels along width of picture

Figure 35: The "cross" pattern is the non-filtered diffraction pattern X-section. camera settings: -b 100 -w 65 -s 1 -F 28 -C 1. z_{down}=downstream pinhole position and a_{down}=downstream pinhole radius, see figure-1. Laser wavelength λ=670 nm.

FILTERED DOWNSTREAM DIFFRACTION PATTERN

Normalized Intensity

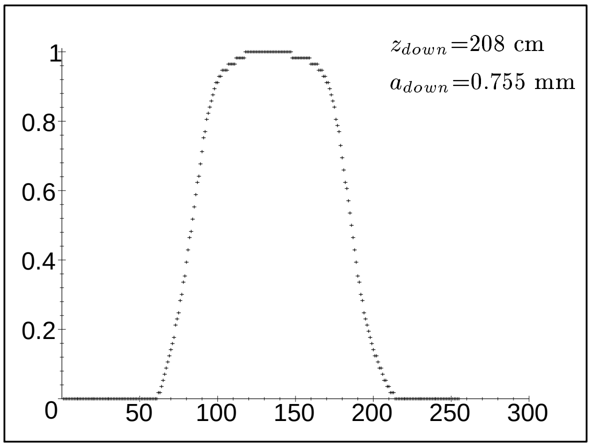

Pixels along width of picture

Figure 36: The "cross" pattern is the filtered diffraction pattern X-section. camera settings: -b 100 -w 65 -s 1 -F 28 -C 1. z_{down}=downstream pinhole position and a_{down}=downstream pinhole radius, see figure-1. Laser wavelength λ=670 nm.

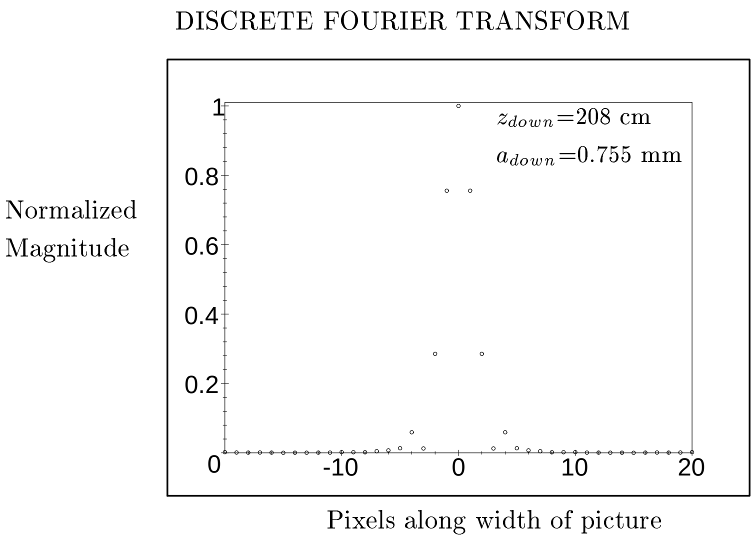

Figure 37: The "cross" pattern is the Discrete Fourier Transform X-section. camera settings: -b 100 -w 65 -s 1 -F 28 -C 1. z_{down}=downstream pinhole position and a_{down}=downstream pinhole radius, see figure-1. Laser wavelength λ=670 nm.

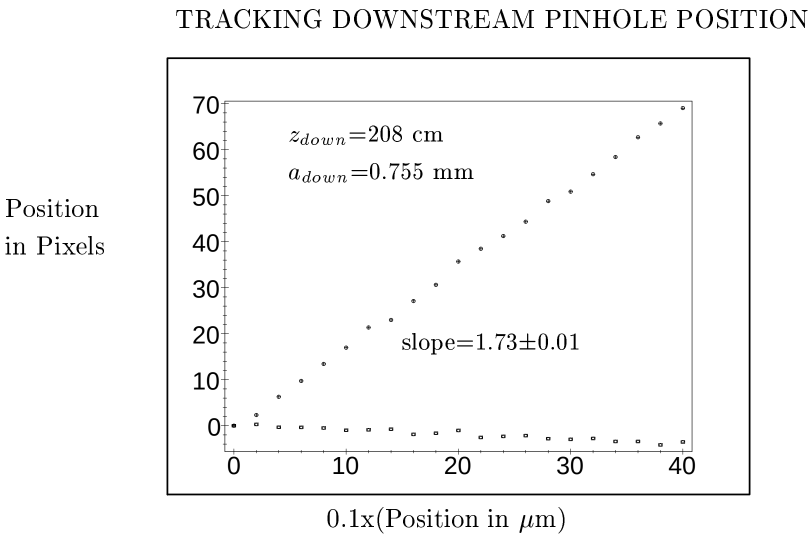

Figure 38: Pinhole moved in increments 20±1 μm along X-axis of the apparatus. Actual displacement is along the X-axis, of the figure above, and measured displacement along the Y-axis. Camera settings: -b 75 -w 94 -s 1 -F 28 -C 1. z_{down}=downstream pinhole position and a_{down}=downstream pinhole radius, see figure-1. Laser wavelength λ=670 nm. "cross-pattern"= X-position of centroid, "circle-pattern"= Phase-shift of first harmonic in X-direction, "box-pattern"= Y-position of centroid, "diamond-pattern"= Phase-shift of first harmonic in Y-direction.

References

[1] Oppenheim, Allan V. and Ronald W. Schafer.**Discrete-Time Signal Processing**. New Jersey: Prentice-Hall Inc., 1989.

[2] Hecht, Eugene **textitSchaum's outlines Optics**. United States: McGraw-Hill Companies, Inc., 1975.

[3] Press, William H., Saul A. Teukolsky, William T. Vetterling and Brian P. Flannery. **Numerical Recipes in C (**$2nd$ **addition)**. New York: Press Syndicate, 1997.